NATIONAL ADVISORY COMMITTEE FOR AERONAUTICS

WARTIME REPORT

ORIGINALLY ISSUED
March 1942 as
Memorandum Report

POWER-ON LONGITUDINAL-STABILITY AND CONTROL TESTS OF THE 1/8-SCALE MODEL OF THE BREWSTER F2A AIRPLANE EQUIPPED WITH FULL-SPAN SLOTTED FLAPS AND A NEW HORIZONTAL TAIL

By John G. Lowry and Thomas A. Toll

Langley Memorial Aeronautical Laboratory
Langley Field, Va.

NACA

WASHINGTON

NATIONAL ADVISORY COMMITTEE FOR AERONAUTICS

MEMORANDUM REPORT

for the

Bureau of Aeronautics, Navy Department

POWER-ON LONGITUDINAL STABILITY AND CONTROL TESTS OF THE 1/8-SCALE MODEL OF THE BREWSTER F2A AIRPLANE EQUIPPED WITH FULL-SPAN SLOTTED FLAPS AND A NEW HORIZONTAL TAIL

By John G. Lowry and Thomas A. Toll

INTRODUCTION

Tests were made in the NACA 7- by 10-foot wind tunnel of the 1/8-scale model of the Brewster F2A airplane equipped with full-span slotted flaps and a new horizontal tail. The object of the tests was to determine the power-on static longitudinal stability and control characteristics of the model with the new horizontal tail. Some additional tests to determine the characteristics of the model, both in free air and near the ground, were made after certain modifications had been made to the horizontal tail.

MODEL AND EQUIPMENT

The 1/8-scale model of the Brewster F2A airplane is the same as that used for the tests reported in references 1 and 2 with the single exception that a new horizontal tail of increased area and higher aspect ratio was installed for the current tests. A three-view drawing of the complete model is presented in figure 1. Photographs of the model as installed in the tunnel are presented in figures 2 and 3. Figure 4 is a detail drawing of the new horizontal tail with a superimposed outline of the plan form of the original horizontal tail. Figure 5 is a comparison drawing of the original horizontal tail, the new horizontal tail, and the two modifications of the latter which were investigated. The original horizontal tail will be known as No. 1 and the unmodified new horizontal tail as No. 2. Horizontal tail No. 3 is the new tail with the trailing edge beveled 15° from the chord line and horizontal tail No. 4 is

the new tail with the trailing edge beveled 10° from the chord line. The modifications of the new tail were made with the view of decreasing elevator hinge moments and were made possible by the thickness of the trailing edge of the elevator as furnished by the Brewster Company.

All dimensions and areas given in figures 1 and 4, with the exception of the new horizontal tail areas and elevator root-mean-square chord, were furnished by the Brewster Company. The areas given for the various horizontal tail components included fuselage area bounded by the projections of the outlines of the respective surfaces. The elevator root-mean-square chord was determined from the elevator area as defined above.

Elevator hinge moments were determined from the twist of a calibrated torque rod extending from the right elevator tip (figs. 2 and 3) to a pointer and dial assembly mounted outside the tunnel wall. To minimize lateral bending and oscillations due to the air stream, the torque rod was enclosed over its entire length in a hollow tube. The tube was of sufficiently large inside diameter to allow freedom of motion of the torque rod. (See fig. 3.)

The angle of attack of the reference thrust line was determined by means of leveling lugs that were fitted into holes previously drilled into the side of the fuselage. The rudder, flap, and aileron angles were set by means of templets furnished with the model. Stabilizer angles were set by means of an inclinometer resting on a stabilizer templet with its surface parallel to the stabilizer chord line. The latter templet and one used to obtain elevator angle settings were made at the NACA Laboratory.

The model was powered by the same electric motor as described in reference 2. The propeller is the same as that used in the tests of reference 3.

Additional equipment was used during tests to determine ground effect. The ground was simulated by a flat wooden plate completely spanning the tunnel and extending several feet ahead of and behind the model. The plate was set parallel to the longitudinal axis of the tunnel and so adjusted in height as to be almost tangent to the wheels of the landing gear when the model was a zero angle of attack. Details of the plate construction and its installation are given in reference 4.

TESTS AND RESULTS

Test conditions.- The tests were made in the NACA 7- by 10-foot wind tunnel. All the tests were run at a dynamic pressure of 16.37 pounds per square foot which corresponds to a velocity of about 80 miles per hour under standard sea-level conditions, and to a test Reynolds number of about 570,000 based on the mean aerodynamic chord of 9.36 inches. The effective Reynolds number, Re, of all tests excluding those with the ground board in place, was 912,000 based on a turbulence factor for the 7- by 10-foot tunnel of 1.6.

Coefficients.- The results of the tests are given in the form of standard NACA coefficients of forces and moments based on model dimensions. All pitching moments are taken about the center-of-gravity location of the complete airplane shown on figure 1. The data are referred to the stability axes as defined in reference 2. The coefficients are defined as follows:

C_{D_R} resultant-drag coefficient $\left(\frac{X}{qS}\right)$

C_L lift coefficient $\left(\frac{L}{qS}\right)$

C_m pitching-moment coefficient about center of gravity $\left(\frac{m}{qSc}\right)$

C_{h_e} elevator hinge-moment coefficient $\left(\frac{H}{qS_e c_{rms}}\right)$

where

X force along X axis; positive when directed backwards

L force along Z axis; positive when directed upwards

m pitching moment about Y axis; positive when it tends to depress the tail

q dynamic pressure $= \frac{1}{2}\rho V^2$ (16.37 pounds per square foot)

S wing area (3.265 square feet)

c mean aerodynamic chord of wing (0.78 foot)

b wing span (4.38 feet)

S_e elevator area (0.311 square foot)

c_{rms} elevator root-mean-square chord (0.172 foot)

H elevator hinge moment, foot-pounds; positive when it tends to depress the elevator trailing edge

The following propeller coefficients are used:

T_c' effective model-thrust coefficient = $\frac{T}{qS}$

T_c effective propeller-thrust coefficient = $\frac{T}{\rho V^2 D^2}$

V/nD advance diameter ratio

where

T effective thrust in pounds

ρ mass density of air in slugs per cubic foot

V airspeed in feet per second

D propeller diameter (1.54 feet)

n propeller speed in revolutions per second

rpm propeller speed in revolutions per minute

Symbols.- Certain symbols are used in the text and figures, and are defined as follows:

α angle of attack of thrust line, degrees

i_t angle of stabilizer setting with respect to thrust line, degrees; positive when trailing edge is down

δ_e elevator deflection (with respect to stabilizer chord), degrees; positive when trailing edge of elevator is moved down

δ_r rudder deflection, degrees; positive when trailing edge of rudder is moved to left

δ_f flap deflection, degrees; positive when trailing edge of flap is moved down

δ_a aileron deflection, degrees; positive when trailing edge of aileron is moved down

δ_t tab deflection with respect to the elevator, degrees; positive when trailing edge of tab is moved down

F_s elevator control stick force, pounds; positive when pilot must pull on stick to resist force

β angle of propeller blade setting measured at the 75 percent radius (20°)

Corrections.- The results have not been corrected for tares caused by the model support.

All the angles of attack, the drag coefficients, and the pitching-moment coefficients have been corrected for the effects of the tunnel walls. The pitching-moment correction applied for the power-on tests takes into account the effect of power on the dynamic pressure in the vicinity of the tail. The jet-boundary corrections applied were computed as follows:

Induced drag correction, $\Delta C_{D_i} = \delta \frac{S}{C} C_L^2$

Induced angle-of-attack correction, $\Delta \alpha_i = \delta \frac{S}{C} C_L (57.3)$

Pitching-moment-coefficient correction,

$$\Delta C_m = 57.3 \times \delta_{a_w} \times \frac{S}{C} \times \frac{dC_m}{di_t} \times C_L \times \sqrt{\frac{q_o}{q_s}}$$

All corrections are added to the tunnel data. In the above equations

δ = 0.115

δ_{a_w} = 0.065

C = tunnel cross-sectional area (69.59 square feet)

$\frac{dC_m}{di_t}$ = change in pitching-moment coefficient per degree change in stabilizer setting

q_o = free-stream dynamic pressure (pounds per square foot)

q_s = dynamic pressure (pounds per square foot) in the vicinity of tail

Test procedure.- Since the propeller and blade angle used in these tests were the same as those used in the tests of reference 3, it was not considered necessary to repeat the propeller-calibration tests which had previously been made. Operating charts were obtained by the same procedure as described in reference 2. Figure 3(a) of reference 2 was again used to obtain the prototype thrust coefficients.

For convenience in locating results, a résumé of the tests is given in the following table:

$\delta_r = \psi = \delta_a = 0^\circ$, $\beta = 20^\circ$

Test no.	Horiz. tail no.	Power condition	$\delta_f{}^\circ$	$\alpha_T{}^\circ$	$i_t{}^\circ$	$\delta_e{}^\circ$	$\delta_t{}^\circ$	Figure no.
40	2	Wind-milling	40	Range	-5	0	0	7
41					5			7
42		Half rated			-5			8
43					5			8
44					-0.5			8,12,15
45						2		12
46						-2		12
47						-5		12
48						-10		12
49		Wind-milling				0		7,11
50						-2		11
51						-5		11
52						-10		11
53						-15		11
54		Half rated		-5.96		-15 to 10		20
55				-1.40				20
56				7.24				20
57				11.00				20
58		Wind-milling		-5.96				20
59				-1.40				20
60				7.24				20
61				11.00				20

Test no.	Horiz. tail no.	Power condition	δ_f°	α_T°	i_t°	δ_e°	δ_t°	Figure no.
62	2	Rated	0	1.41	-0.5	-15 to 10	0	19
63				5.20				19
64				9.88				19,21
65				12.37				19
66		Wind-milling		1.41				19
67				5.20				19
68				9.88				19,21
69				12.37				19
70		Rated		Range		0		6,10
71						-2		10
72						2		10
73		Wind-milling				0		9
74						2		9
75						-2		9
76						-5		9
77		Rated			-5.0	0		6
78					5.0			6
79	3				-0.5	-15 to 10		21
80	4			1.41				22
81				9.88				21,22,25
82				12.37				22
83		Wind-milling		1.41				22
84				9.88				21,22,25
85				12.37				22

Test no.	Horiz. tail no.	Power condition	δ_f °	α_T °	i_t °	δ_e °	δ_t °	Figure no.
86	4	Rated	0	Range	-0.5	0	0	13
87						-2		13
88						-5		13
89		Half rated	40			0		14,15
90						-5		14
91				-5.96		-15 to 10		23
92				-1.40				23,25
93				11.00				23,24
94		Rated		-2.80				25
95		Wind-milling		-5.96				23
96				-1.40				23,25
97				11.00				23,24
98		Half rated					-10	24
99							10	24
100		Wind-milling					-10	24
101							10	24
[a]104				Range		0	0	16
105						-10		16
106						-20		16
107						-25		16
108						-30		16
109						No horiz. tail		

[a]Tests 104 to 109 made with ground board in tunnel.

DISCUSSION

Effect of stabilizer.- To facilitate a comparison of the three tails, numerical values of some of the important criteria at a lift coefficient of 1.0 are presented in table I.

The stabilizer tests show that the change in pitching-moment coefficient with stabilizer angle ($\partial C_m/\partial i_t$) not only increases with the application of power, but also increases somewhat with lift coefficient in power-on tests (figs. 6, 7, and 8). The values of $\partial C_m/\partial i_t$ for horizontal tail No. 2 are slightly greater than the values for horizontal tail No. 1. (See table I or references 2 and 3.)

As previously pointed out and discussed in reference 3, the slope of the pitching-moment curve ($\partial C_m/\partial C_L$) becomes more negative with increased positive deflection of the elevator or stabilizer.

Effect of elevator.- A comparison of figures 9-14 with results presented in references 2 and 3 shows that the new elevators have very nearly the same effectiveness, $\partial C_m/\partial \delta_e$, as the original elevators, horizontal tail No. 1. (See table I.) The new tail, in its original or modified forms (horizontal tails Nos. 2 and 4) provides greater longitudinal stability, $\partial C_m/\partial C_L$, than that reported in references 2 and 3 (fig. 15).

To determine the ability of the pilot to get the tail of the airplane down in landing, calculations of the ground effect were made at the Laboratory. Since the results indicated high elevator angles, an additional series of tests of the model with horizontal tail No. 4 was made with a ground board in the tunnel and at a level about 1/4 inch below the front wheels of the model at zero angle of attack. The ground board tests were made with propeller windmilling and flaps deflected. It may be seen from figure 16 that the elevator effectiveness drops off considerably at the high elevator deflections which would be required to trim the airplane for high lift coefficients. At a value of $C_L = 2.0$, the elevator effectiveness, $\partial C_m/\partial \delta_e$, is -0.0162 for elevator angles between 0° and -10° but at elevator angles between 25° and 30°, $\partial C_m/\partial \delta_e$ is only about -0.006.

The change in elevator angle required to trim the powered model throughout the lift range is about twice as great for horizontal tails Nos. 2 and 4 as for horizontal tail No. 1. (See figs. 17 and 18.) With propeller windmilling, the change in elevator angle to trim throughout the lift range is considerably greater than when the model motor is developing rated power. The increased effectiveness of the new horizontal tail is apparent from a comparison of figure 17 with figure 18 where the change in elevator angle for trim at a given lift coefficient from flap retracted condition (fig. 17) to flap deflected condition (fig. 18) is considerably greater for the model equipped with horizontal tail No. 1 than with horizontal tails Nos. 2 and 4.

The curve representing the model above the ground board shows that considerably larger elevator angles are required at any given lift coefficient in landing than in free air. It seems, however, that little difficulty should be experienced in getting the tail down for landing at values of C_L as high as 2.2, or possibly higher, provided the center of gravity is not moved forward of the position indicated for the model in figure 1. A slight rearward movement of the center of gravity from its present location would seem advisable from considerations of getting the tail down for landing.

Elevator hinge-moment coefficients.- The change in elevator-hinge-moment coefficient with elevator deflection, $\partial C_{h_e}/\partial \delta_e$, is about constant for the windmilling condition throughout the range of elevator deflections and angles of attack tested and $\partial C_h/\partial \alpha$ has an almost constant negative value. (See figs. 19 and 20.) For the power-on conditions, however, the values of $dC_h/d\delta_e$ increase with increased positive angles of attack probably because of the increased velocity at the tail. With flaps retracted and rated power, $\partial C_h/\partial \alpha$ is positive for high negative elevator angles and negative for all elevator angles on the positive side of -4°. For the half-power flaps-deflected condition, $\partial C_h/\partial \alpha$, is negative for all values of δ_e on the positive side of -13°. Some numerical values of $\partial C_h/\partial \delta_e$ and $\partial C_h/\partial \alpha$ are given in table I.

After completing the tests of the new horizontal tail, attempts were made to reduce the elevator hinge moments by beveling the elevator trailing edge. The first modification (horizontal tail no. 3) involved a 15° bevel from the chord line. The single test made of this modified form showed that the elevator was overbalanced in the vicinity of 0° deflection. (See fig. 21.) A tendency of the elevator to flutter at this angle was observed during the test.

As the above modification seemed unsatisfactory the bevel angle was changed to 10° from the chord line (horizontal tail No. 4). A comparison of the hinge-moment-coefficient characteristics of the original new tail and its two modified forms is presented in figure 21 for the model at angle of attack of 10.04°. A comparison of figures 22 and 23 with figures 19 and 20 shows that the hinge-moment coefficients, and the values of $\partial C_{h_e}/\partial \delta_e$, are considerably less for horizontal tail No. 4 than for horizontal tail No. 2 over a large portion of the range of elevator deflections tested. Values of $\partial C_{h_e}/\partial \alpha$ for horizontal tail No. 4 change from positive to negative at about zero elevator angle for the rated-power condition with flaps retracted. The parameter $\partial C_{h_e}/\partial \alpha$ remains negative for all elevator deflections for the condition of half-rated power with flaps deflected.

The results of tab tests of horizontal tail No. 4 (fig. 24) show the tab to be very effective in changing the elevator hinge-moment coefficients. Numerical values of $\partial C_{h_e}/\partial \delta_t$ are given in table I. It appears that the tab angle required to trim out the elevator hinge moment would not be greater than $\pm 10°$ at any value of C_L which might be obtained with flaps retracted. For the high lift coefficients experienced with the flaps extended, as much as 20° tab angle might be required for trim.

The hinge-moment coefficients with rated power (fig. 25) are usually considerably higher than the values for the windmilling condition. This does not mean, however, that the stick forces would increase with power, since elevator effectiveness increases at about the same rate as the elevator hinge-moment.

The variation of elevator-stick force which would be required to trim the F2A airplane while changing from the flaps retracted condition to flaps deflected at a lift coefficient of 1.0 is shown in figure 26. Force calculations are based on a gross weight of the airplane of 6600 pounds. The forces are assumed to be trimmed to zero at a lift coefficient of 1.0 with the flaps retracted. A comparison of the curves representing horizontal tails Nos. 2 and 4 indicates that considerably lower forces would be expected for the airplane equipped with the modified tail, No. 4.

CONCLUDING REMARKS

From the data obtained it appears that the F2A airplane with the new horizontal tail will give satisfactory stability and control

characteristics with full-span slotted flaps. Some improvement in control might be obtained by a slight rearward movement of the center-of-gravity location.

If the trailing edge of the prototype elevator is intended to be relatively thick, as was that of the model elevator, it appears that the stick forces may be reduced considerably by beveling the trailing edge. If, however, the trailing edge is to be of normal thickness, it may be expected that the stick forces will be somewhat lower than those indicated from the tests of horizontal tail No. 2.

Langley Memorial Aeronautical Laboratory,
National Advisory Committee for Aeronautics,
Langley Field, Va., March 14, 1942.

REFERENCES

1. Lowry, John G.: Power-Off Wind-Tunnel Tests of the 1/8-Scale Model of the Brewster F2A Airplane. NACA MR, June 21, 1941.

2. Lowry, John G.: Power-On Wind-Tunnel Tests of the 1/8-Scale Model of the Brewster F2A Airplane with Full-Span Slotted Flaps. NACA MR, Aug. 21, 1941.

3. Lowry, John G.: Additional Power-On Wind-Tunnel Tests of the 1/8-Scale Model of the Brewster F2A Airplane with Full-Span Slotted Flaps. NACA MR, Oct. 27, 1941.

4. Recant, I. G.: Plate Method of Ground Representation for Wind-Tunnel Determination of Elevator Effectiveness in Landing. NACA TN No. 823, 1941.

L-709

Table I

Lift coefficient, $C_L = 1.0$				
Power and flap condition		Horiz. tail No. 1 (a)	Horiz. tail No. 2	Horiz. tail No. 4
Windmilling propeller $\delta_f = 0°$	$\partial C_m/\partial C_L$	—	-.160	—
	$\partial C_m/\partial i_t$	—	—	—
	$\partial C_m/\partial \delta_e$	—	-.019	—
	$\partial C_h/\partial \delta_e$	—	-.0059	-.0023
	$\partial C_h/\partial \delta_T$	—	—	—
	$\partial C_h/\partial \alpha$	—	-.0015	0
Rated power $\delta_f = 0°$	$\partial C_m/\partial C_L$	-.030	-.108	-.082
	$\partial C_m/\partial i_t$	—	-.041	—
	$\partial C_m/\partial \delta_e$	-.035	-.033	-.031
	$\partial C_h/\partial \delta_e$	—	-.0099	-.0028
	$\partial C_h/\partial \delta_T$	—	—	—
	$\partial C_h/\partial \alpha$	—	-.0022	+.0007
Windmilling propeller $\delta_f = 40°$	$\partial C_m/\partial C_L$	-.097	-.120	—
	$\partial C_m/\partial i_t$	-.022	-.025	—
	$\partial C_m/\partial \delta_e$	—	-.016	—
	$\partial C_h/\partial \delta_e$	—	-.0065	-.0036
	$\partial C_h/\partial \delta_T$	—	—	-.0025
	$\partial C_h/\partial \alpha$	—	-.0024	0
Half-rated power $\delta_f = 40°$	$\partial C_m/\partial C_L$	-.055	-.076	-.067
	$\partial C_m/\partial i_t$	-.029	-.032	—
	$\partial C_m/\partial \delta_e$	-.023	-.021	-.021
	$\partial C_h/\partial \delta_e$	—	-.0089	-.0044
	$\partial C_h/\partial \delta_T$	—	—	-.0056
	$\partial C_h/\partial \alpha$	—	-.0017	-.0008

(a) References 2 and 3

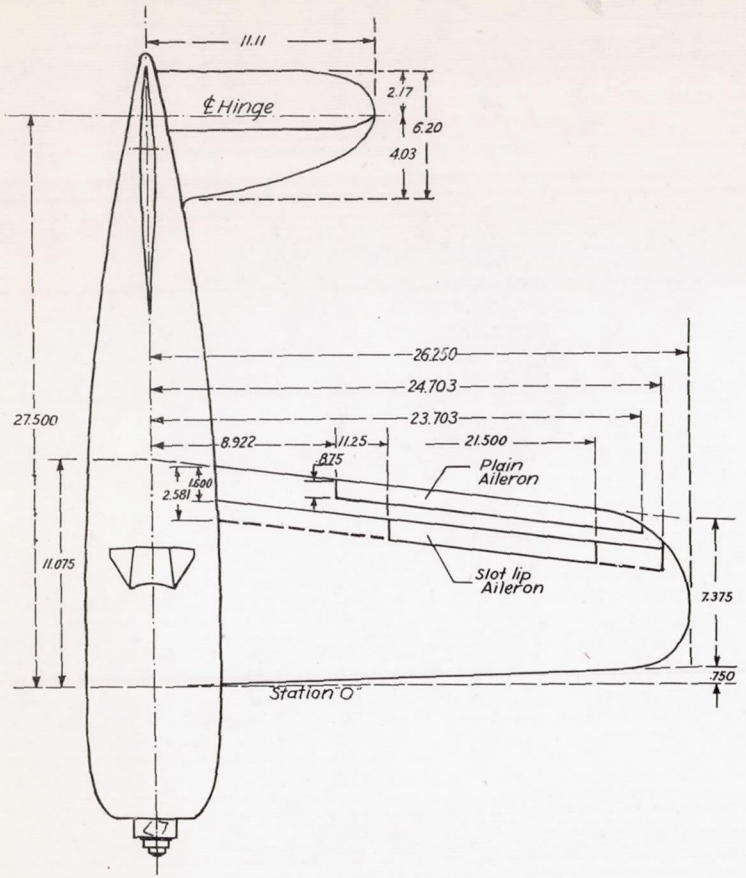

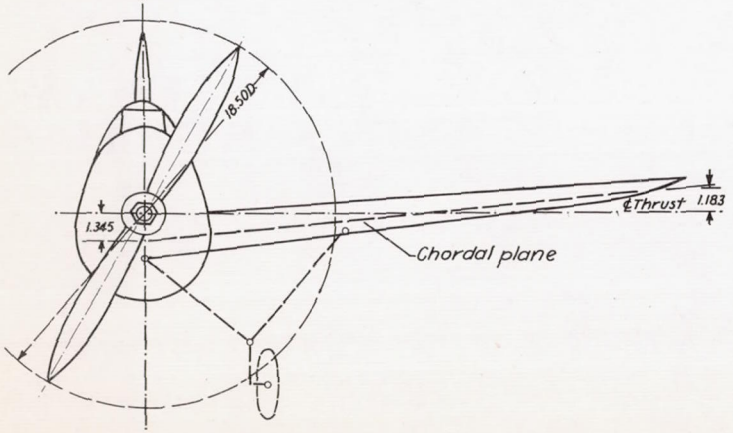

CONSTANTS OF F2A AIRPLANE.

GROSS WEIGHT . . . . . 6600 LBS.
SPAN . . . . . 35.00 FT.
MEAN AERODYNAMIC CHORD 6.24 FT.
AREAS:- WINGS, INCLUDING AILERON. 208.9 SQ.FT.

STABILIZER 30.40 SQ.FT.,
ELEVATOR 19.90 SQ.FT.-TOTAL 50.30 SQ.FT.
ELEVATOR ROOT MEAN SQ.CHORD 1.376 FT.

CG LOCATION (MODEL)
NORMAL FIGHTER, LANDING GEAR RETRACTED

ARM FROM STA. "0"	ARM FROM ℄ THRUST.
2.700 IN.	+.0375 IN.

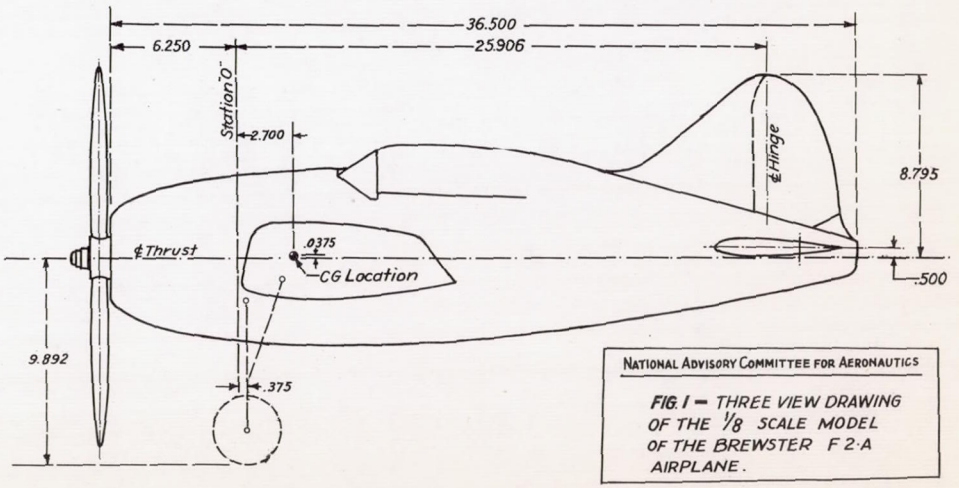

NATIONAL ADVISORY COMMITTEE FOR AERONAUTICS

FIG. 1 — THREE VIEW DRAWING OF THE 1/8 SCALE MODEL OF THE BREWSTER F 2-A AIRPLANE.

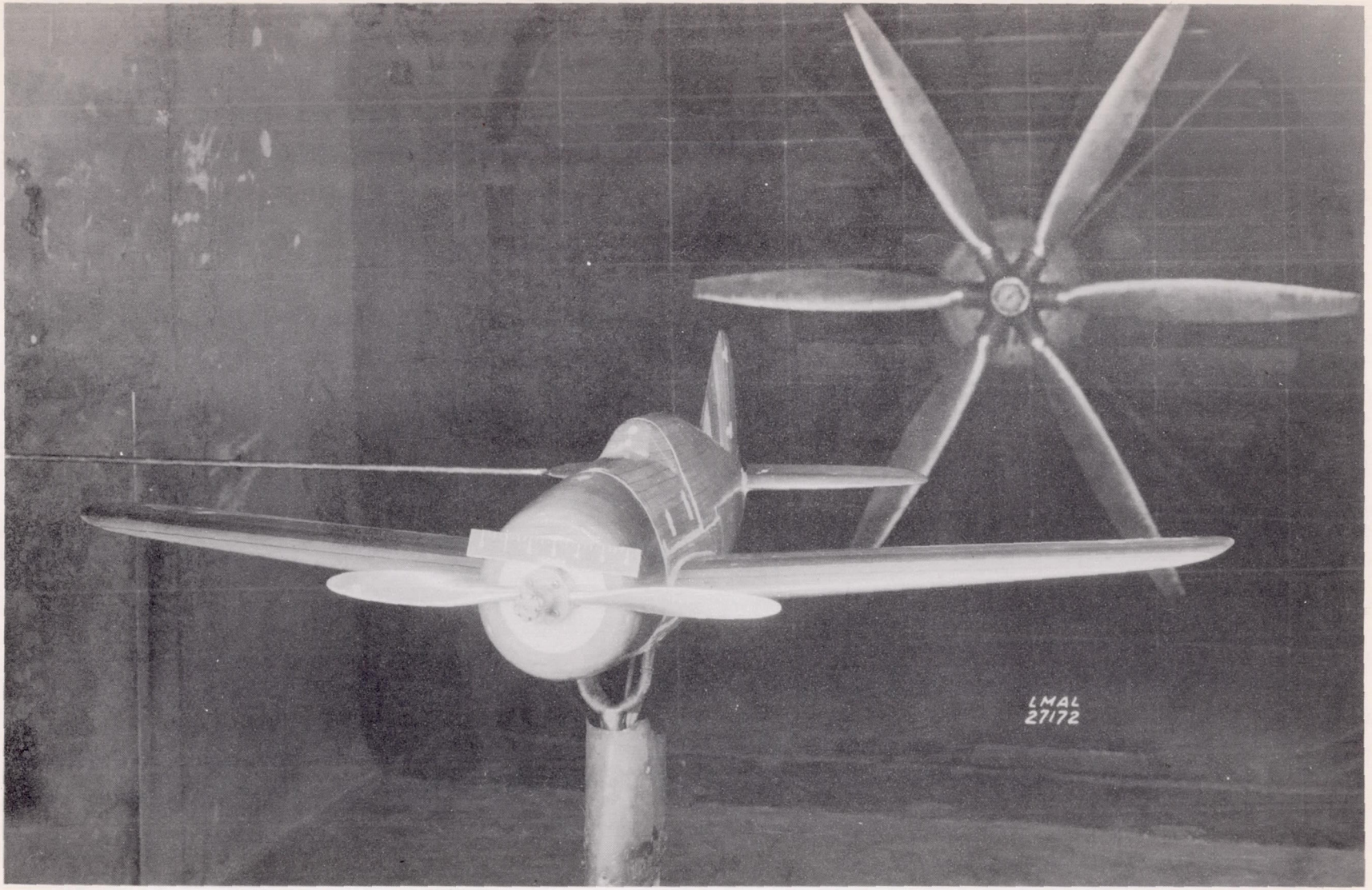

Figure 2.- Three-quarter front view of the $\frac{1}{8}$-scale model of the Brewster F2A airplane in the 7- by 10-foot wind tunnel; flap retracted; landing gear retracted.

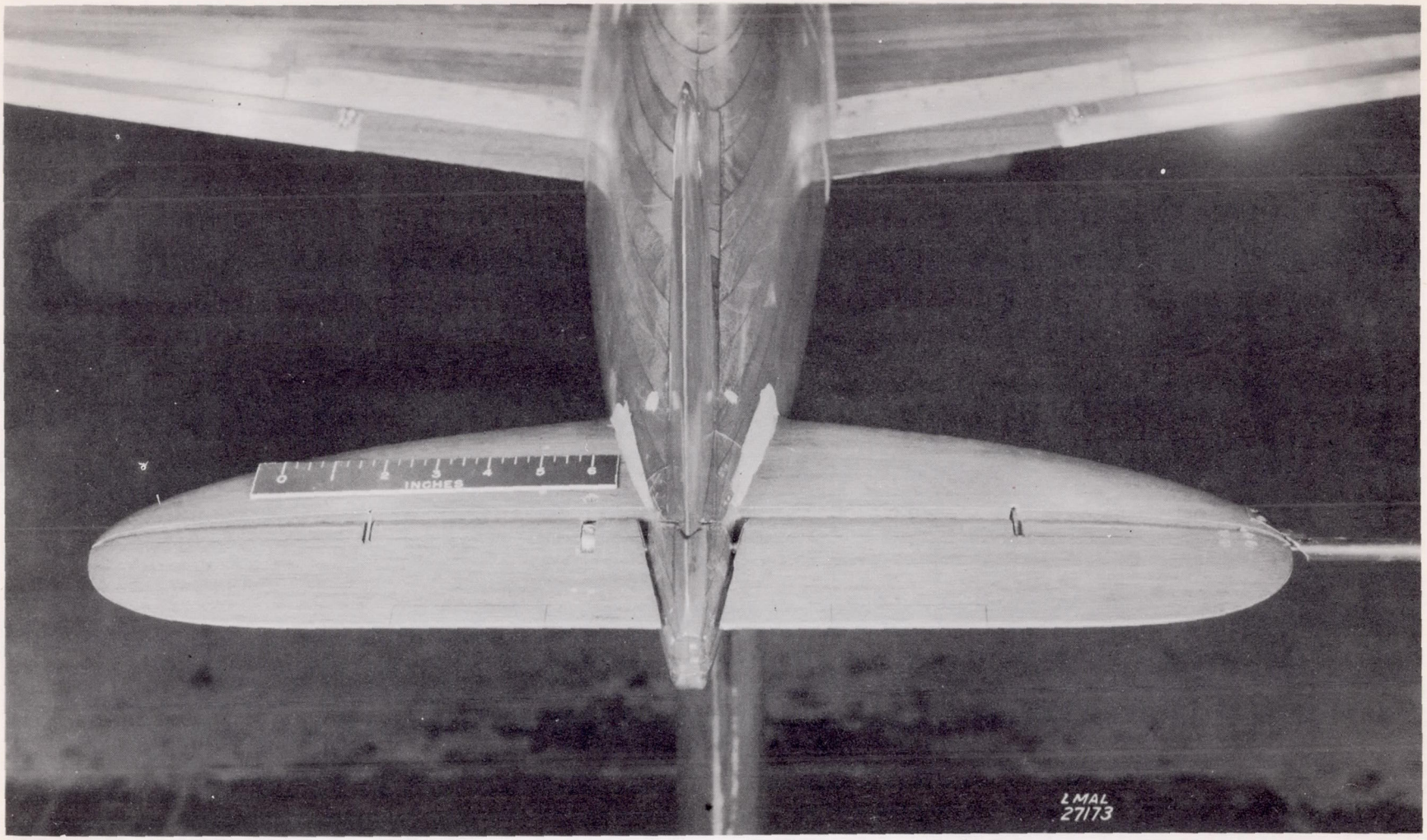

Figure 3.- Horizontal tail surfaces and torque rod attachment of the $\frac{1}{8}$-scale model of the Brewster F2A airplane.

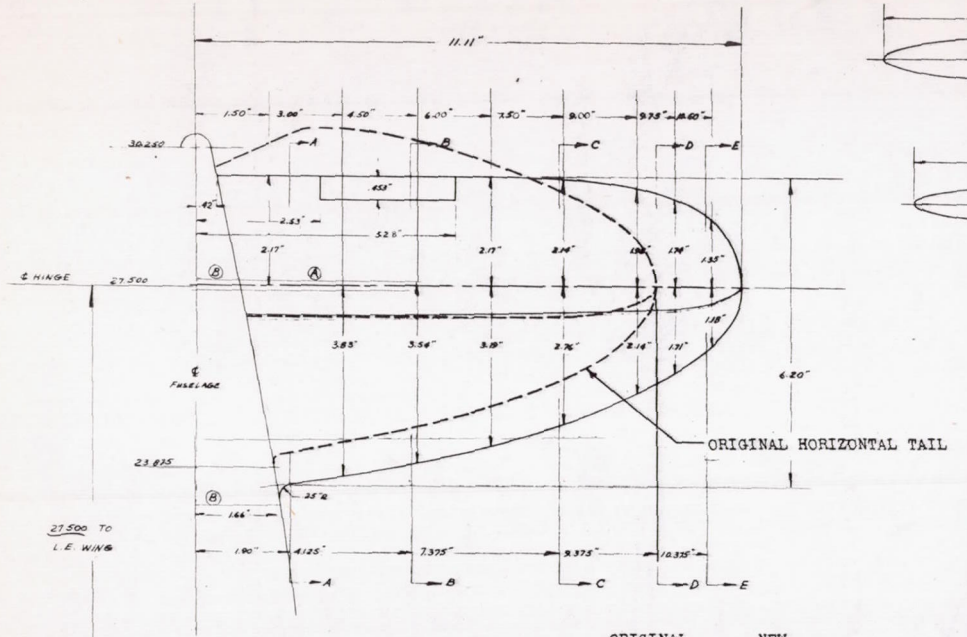

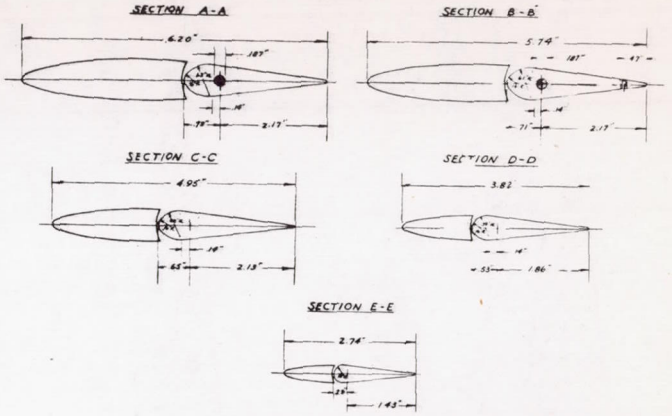

	ORIGINAL TAIL	NEW TAIL
STABILIZER AREA ----------	0.336 sq.ft.	0.475 sq.ft.
ELEVATOR AREA ----------	.313 sq.ft.	.311 sq.ft.
TOTAL AREA ----------	.649 sq.ft.	.786 sq.ft.
ELEVATOR ROOT MEAN SQUARE CHORD--		.172 feet

(All areas include fuselage area)

NATIONAL ADVISORY
COMMITTEE FOR AERONAUTICS

FIGURE 4.- DETAIL DRAWING OF THE NEW H SURFACES OF THE 1/8 SCALE MODEL OF THE F2A AIRPLANE.

HORIZONTAL TAIL ORDINATES

A-A			B-B			C-C			D-D			E-E		
X	y_u	y_l	X	y_u	y_l	X	y_u	y_l	X	y_u	y_l	X	y_u	y_l
L.E. Rad. = .025			L.E. Rad. = .024			L.E. Rad. = .020			L.E. Rad. = .016			L.E. Rad. = .011		
0	0	0	0	0	0	0	0	0	0	0	0	0	0	0
.016	.034	.034	.014	.032	.032	.012	.027	.027	.010	.021	.021	.007	.015	.015
.031	.052	.052	.029	.048	.048	.025	.042	.042	.019	.032	.032	.014	.023	.023
.047	.065	.065	.043	.060	.060	.037	.052	.052	.029	.040	.040	.021	.029	.029
.062	.076	.076	.057	.071	.071	.050	.061	.061	.038	.047	.047	.027	.034	.034
.078	.087	.087	.072	.080	.080	.062	.069	.069	.048	.053	.053	.034	.038	.038
.155	.125	.125	.144	.115	.115	.124	.099	.099	.096	.077	.077	.069	.055	.055
.310	.182	.182	.287	.168	.168	.248	.145	.145	.191	.112	.112	.137	.080	.080
.465	.221	.221	.431	.205	.205	.371	.177	.177	.287	.136	.136	.206	.098	.098
0.62	.255	.255	0.57	.236	.236	0.50	.203	.203	0.38	.157	.157	.274	.113	.113
0.93	.306	.306	0.86	.284	.284	0.74	.245	.245	0.57	.189	.189	.411	.135	.135
1.24	.356	.356	1.15	.320	.320	0.99	.276	.276	0.76	.213	.213	.548	.153	.153
1.86	.384	.384	1.72	.356	.356	1.49	.307	.307	1.15	.237	.237	0.82	.170	.170
2.48	.356	.396	2.30	.366	.366	1.98	.316	.316	1.53	.244	.244	1.10	.175	.175
3.10	.376	.376	2.87	.348	.348	2.48	.300	.300	1.91	.231	.231	1.37	.166	.166
3.72	.331	.331	3.44	.307	.307	2.97	.264	.264	2.29	.204	.204	1.64	.146	.146
4.34	.265	.265	4.02	.246	.246	3.47	.212	.212	2.67	.163	.163	1.92	.117	.117
4.96	.190	.190	4.59	.176	.176	3.96	.152	.152	3.06	.117	.117	2.19	.084	.084
5.58	.105	.105	5.17	.097	.097	4.46	.084	.084	3.44	.065	.065	2.47	.046	.046
5.89	.058	.058	5.45	.054	.054	4.70	.047	.047	3.63	.036	.036	2.60	.026	.026
6.20	0	0	5.74	0	0	4.95	0	0	3.82	0	0	2.74	0	0
T.E. Rad. = .009			T.E. Rad. = .008			T.E. Rad. = .007			T.E. Rad. = .006			T.E. Rad. = .004		

BREWSTER AERONAUTICAL CORPORATION 24-00621

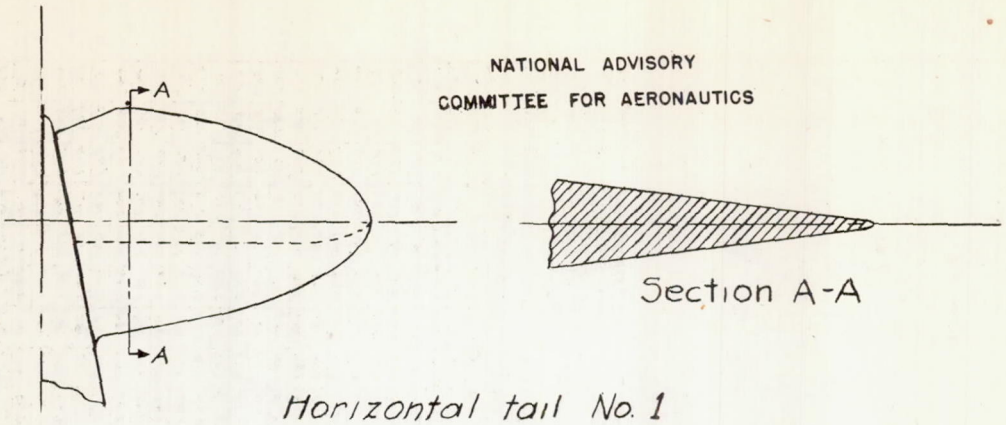

Horizontal tail No. 1

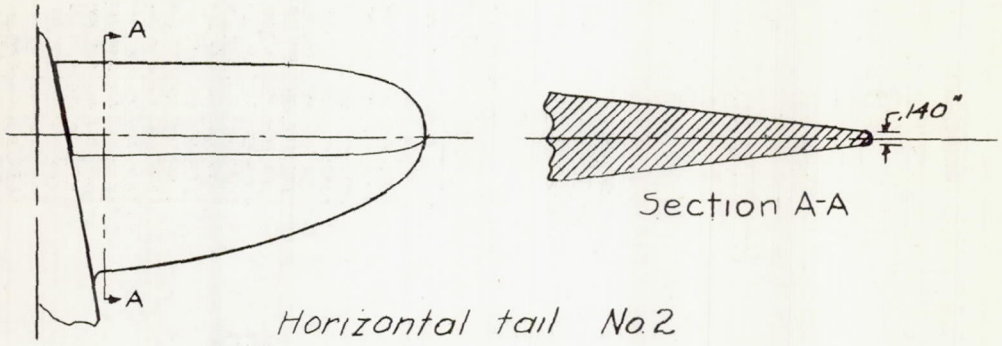

Horizontal tail No. 2

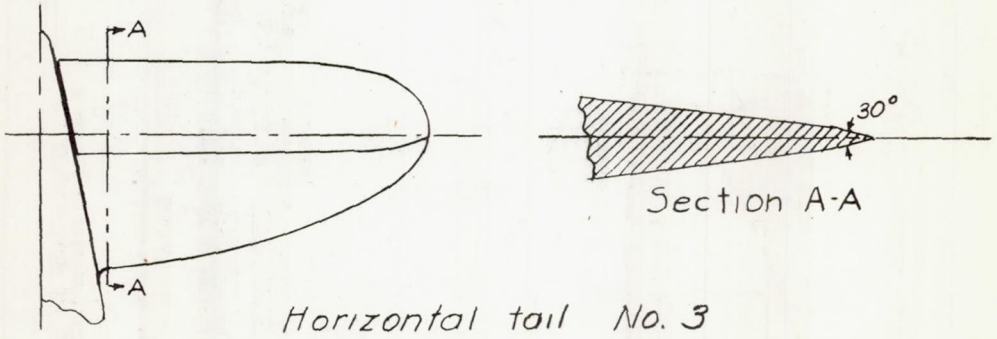

Horizontal tail No. 3

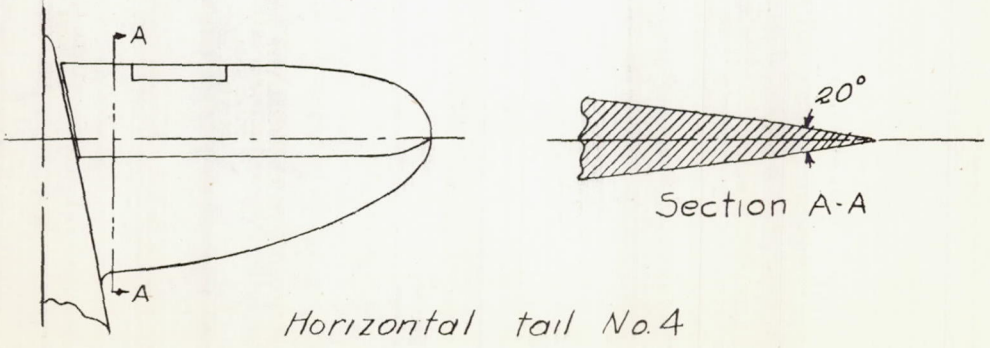

Horizontal tail No. 4

FIGURE 5.- Horizontal tail surfaces investigated.

L-709

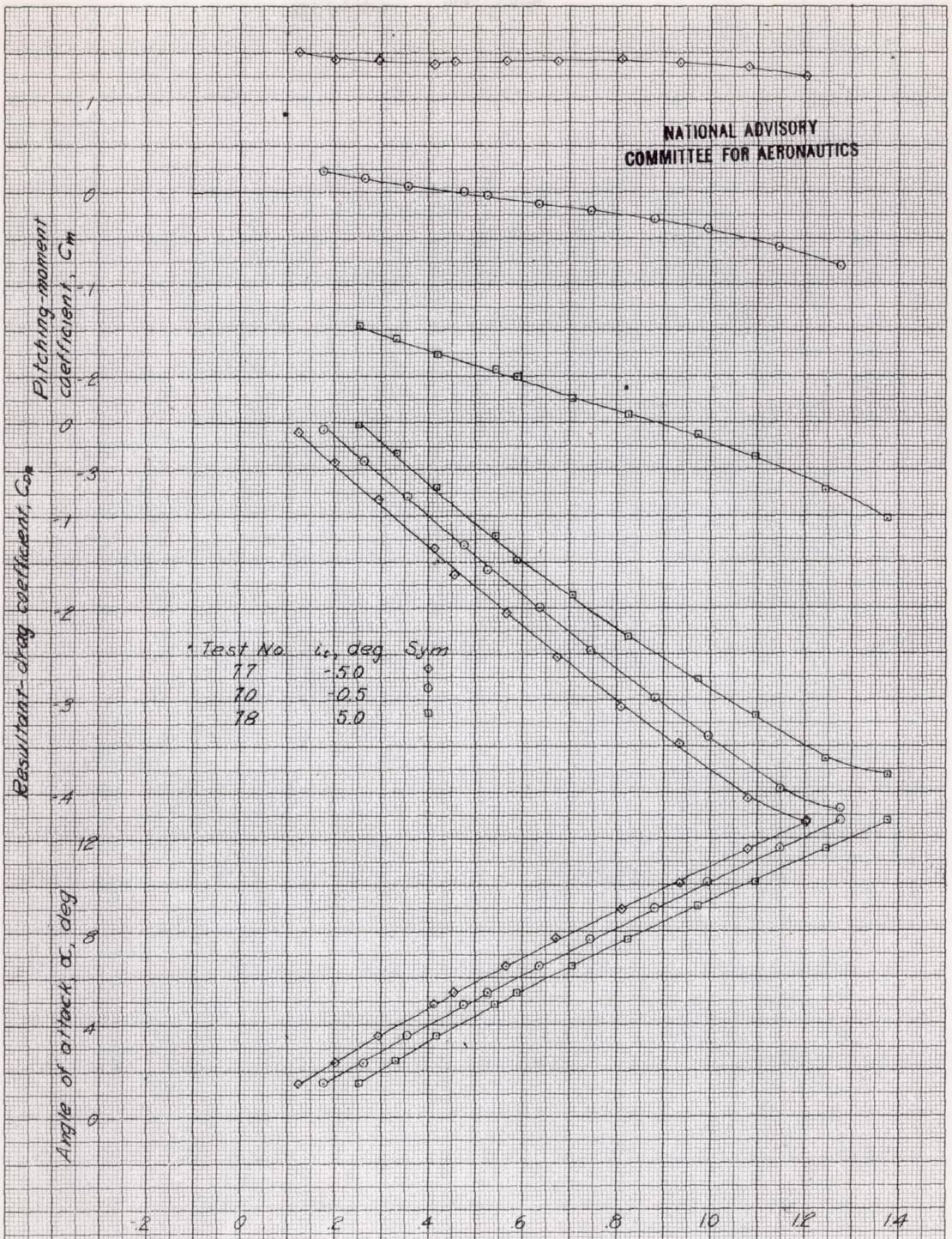

Figure 6. - Effect of stabilizer setting on the aerodynamic characteristics of the 1/8-scale model of the Brewster F2A airplane equipped with horizontal tail No. 2. Approximately rated power, 2-blade propeller, $\beta = 20°$, $\psi = \delta_r = \delta_a = \delta_e = 0°$, $q = 16.37$ lbs/sq ft, $\delta_f = 0°$, landing gear retracted.

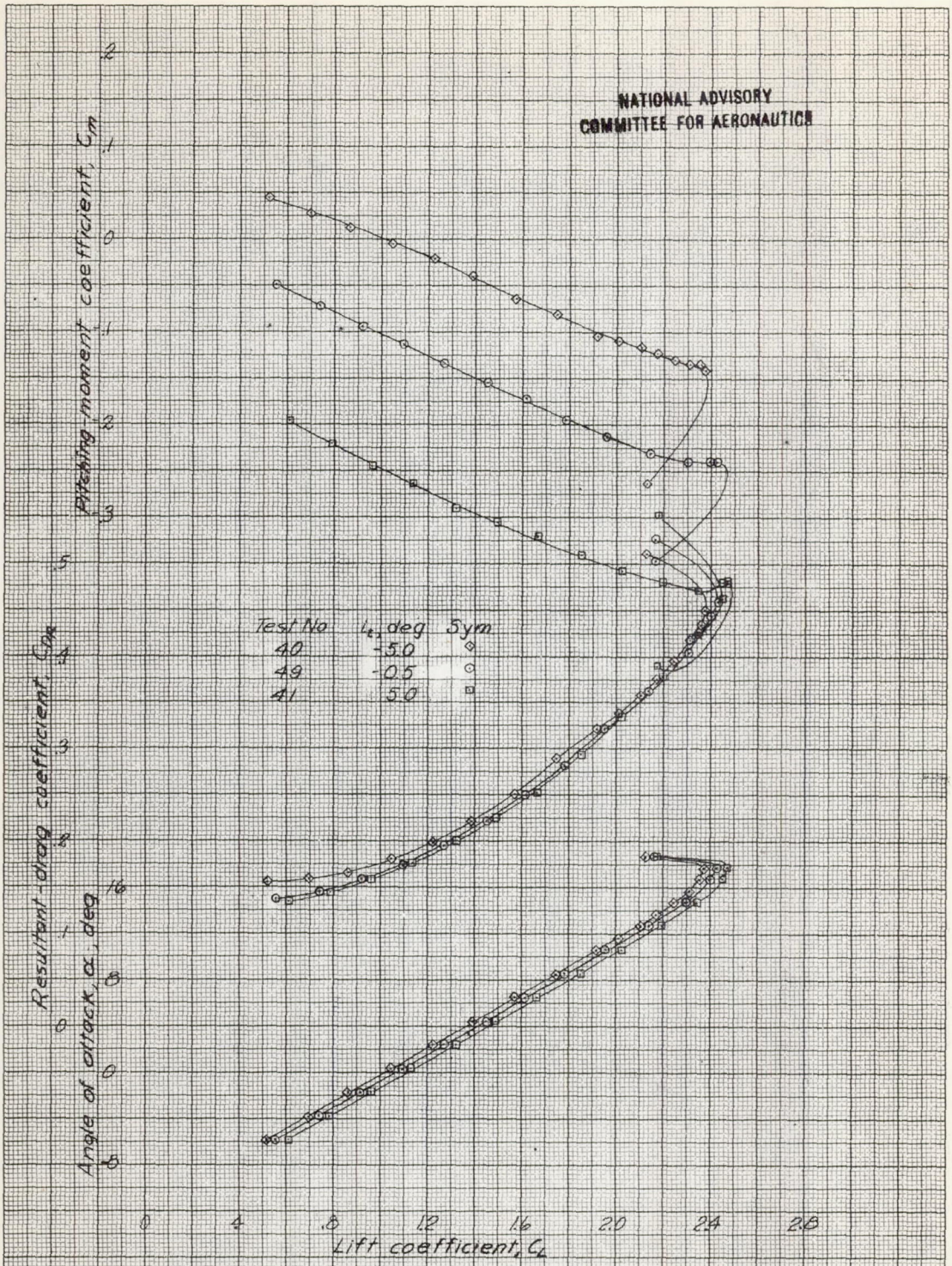

Figure 7. - Effect of stabilizer setting on the aerodynamic characteristics of the 1/8-scale model of the Brewster F2A airplane equipped with horizontal tail No 2. Windmilling propeller , 2-blade propeller, $\beta = 20°$, $\psi = \delta_r = \delta_a = \delta_e = 0°$; $q = 16.37$ lbs/sq ft., $\delta_f = 40°$, landing gear extended.

L-709.

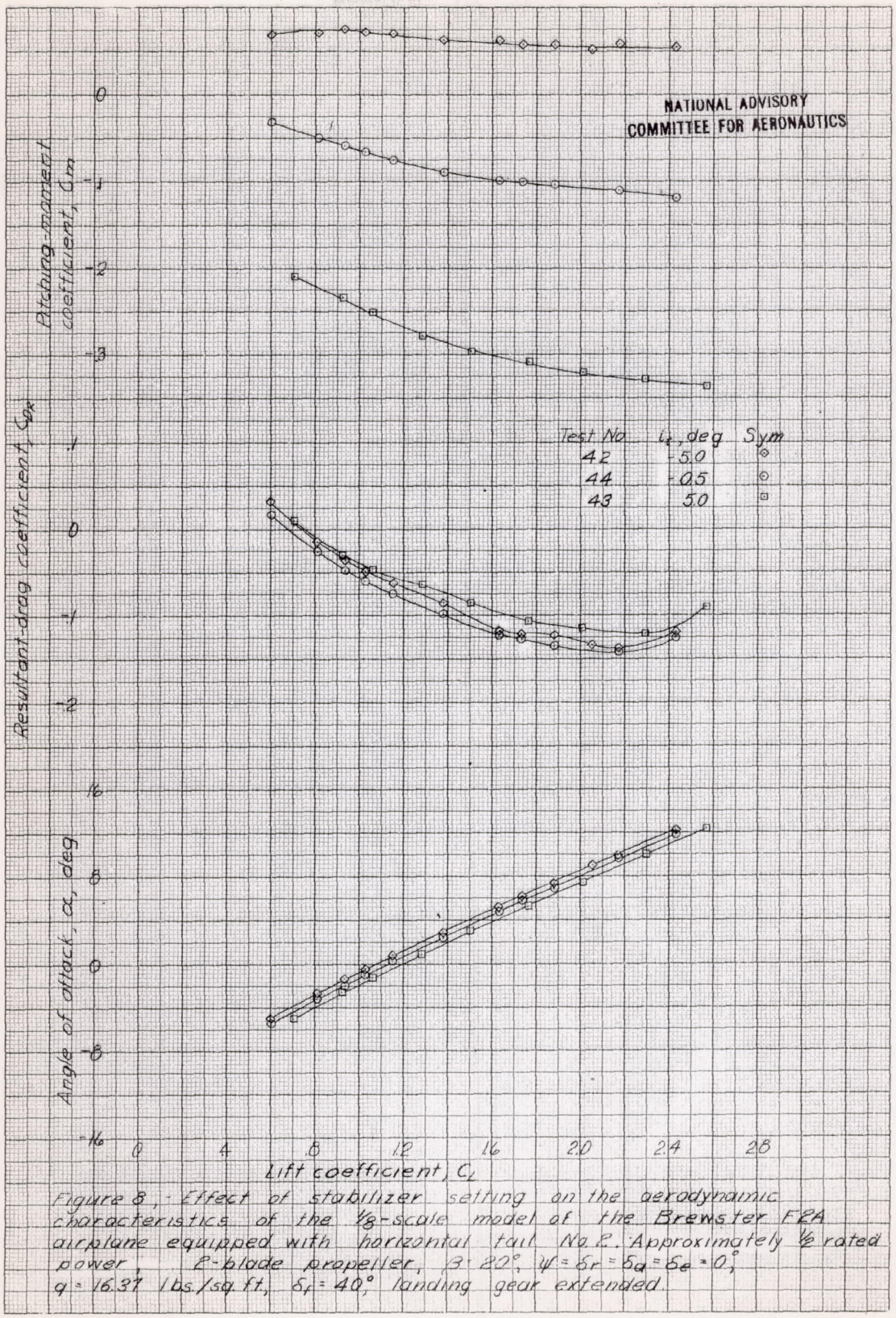

Figure 8.- Effect of stabilizer setting on the aerodynamic characteristics of the 1/8-scale model of the Brewster F2A airplane equipped with horizontal tail No. 2. Approximately 1/2 rated power, 2-blade propeller, $\beta = 20°$, $\psi = \delta_r = \delta_a = \delta_e = 0°$, $q = 16.37$ lbs./sq. ft., $\delta_f = 40°$, landing gear extended.

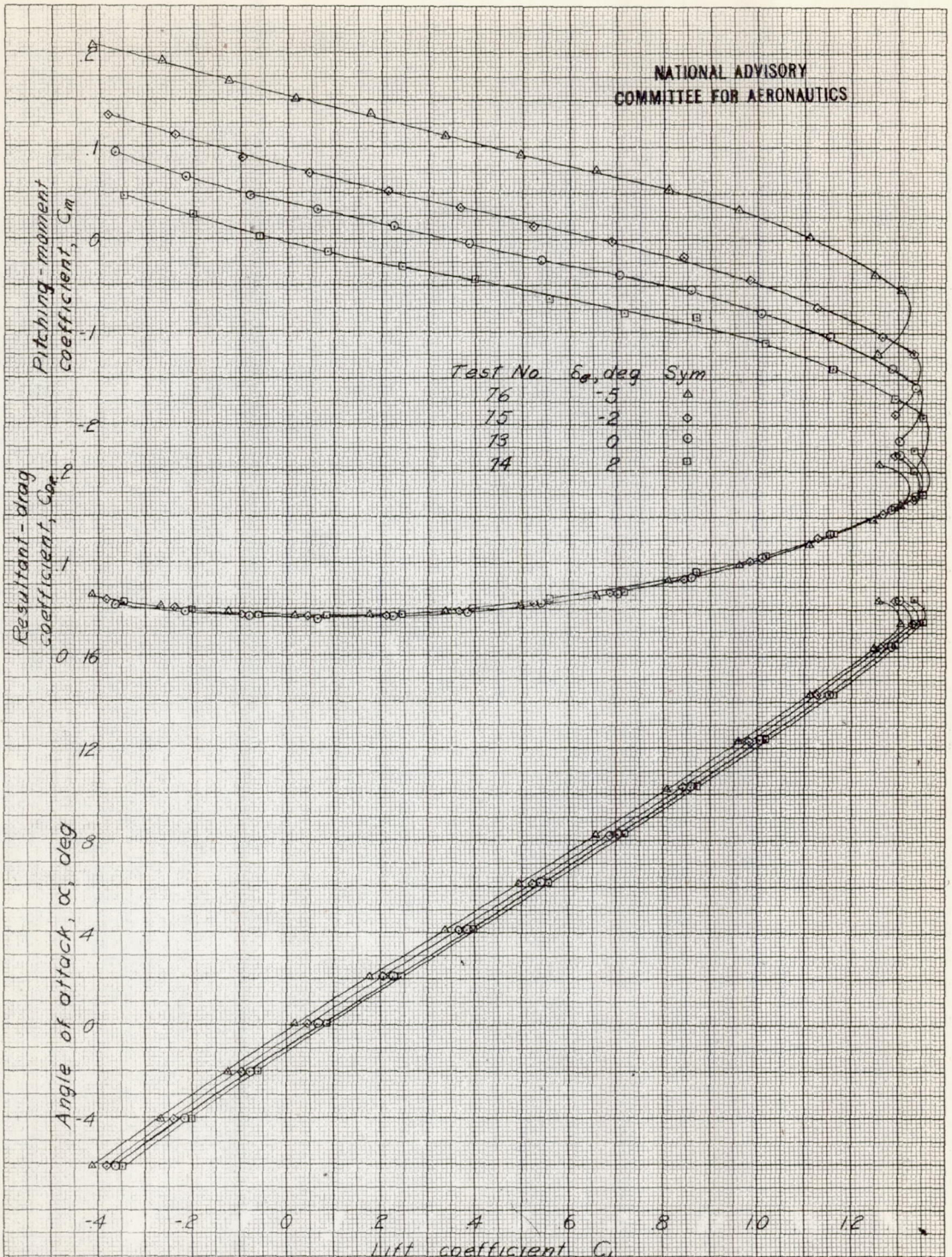

Figure 9.- Effect of elevator deflection on the aerodynamic characteristics of the 1/8-scale model of the Brewster F2A airplane equipped with horizontal tail No. 2. Windmilling propeller, 2-blade propeller, $R = 2.0$; $i_t = \delta_f = \delta_a = 0°$, $i_t = -0.5°$; $q = 16.37$ lbs./sq. ft., $\delta_f = 0°$, landing gear retracted.

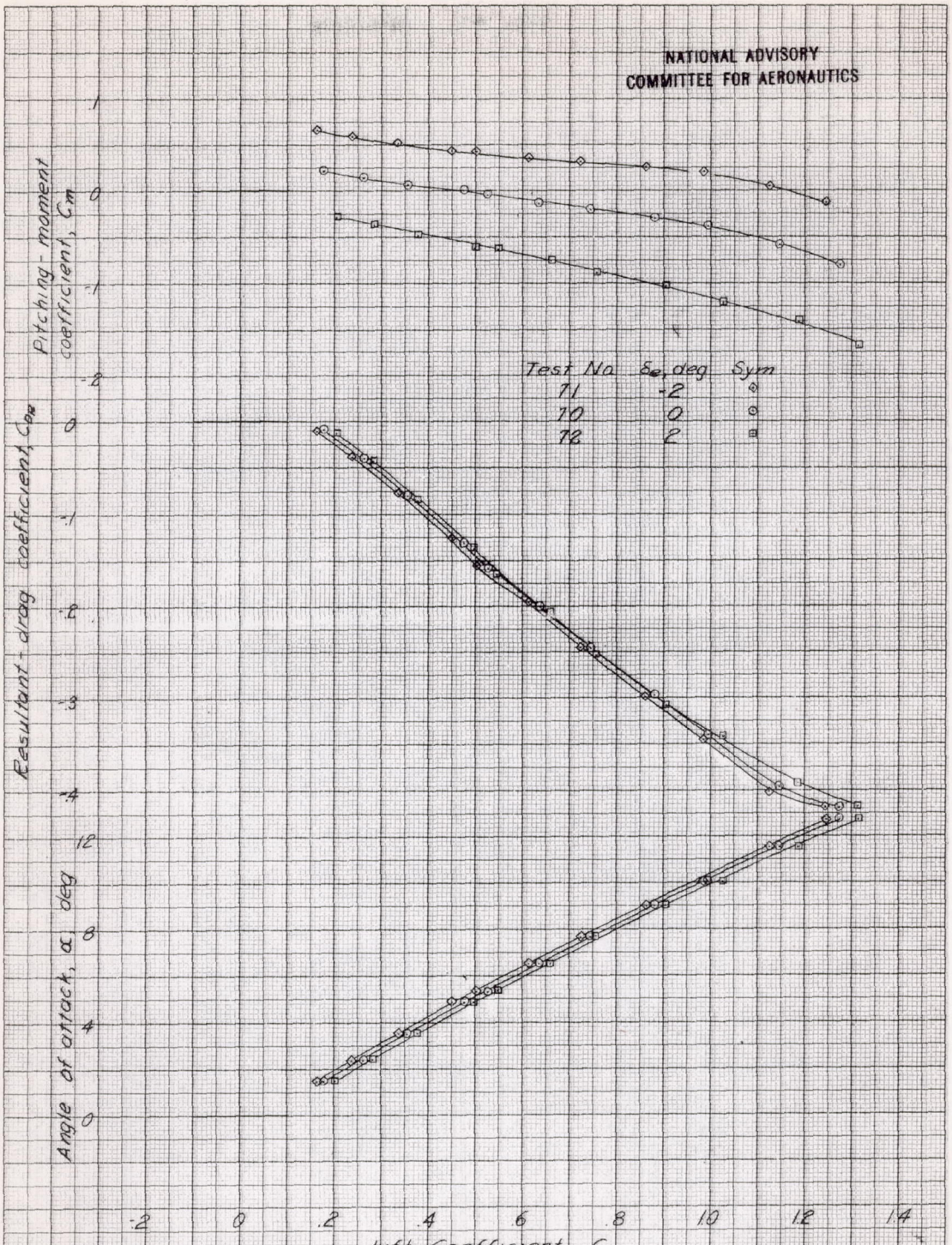

Figure 10.- Effect of elevator deflection on the aerodynamic characteristics of the 1/3-scale model of the Brewster F2A airplane equipped with horizontal tail No. 2. Approximately rated power. 2-blade propeller, $\beta = 20°$, $\psi = \delta_r = \delta_a = 0°$, $i_t = -0.5°$, $q = 16.37$ lbs/sq ft, $\delta_f = 0°$, landing gear retracted.

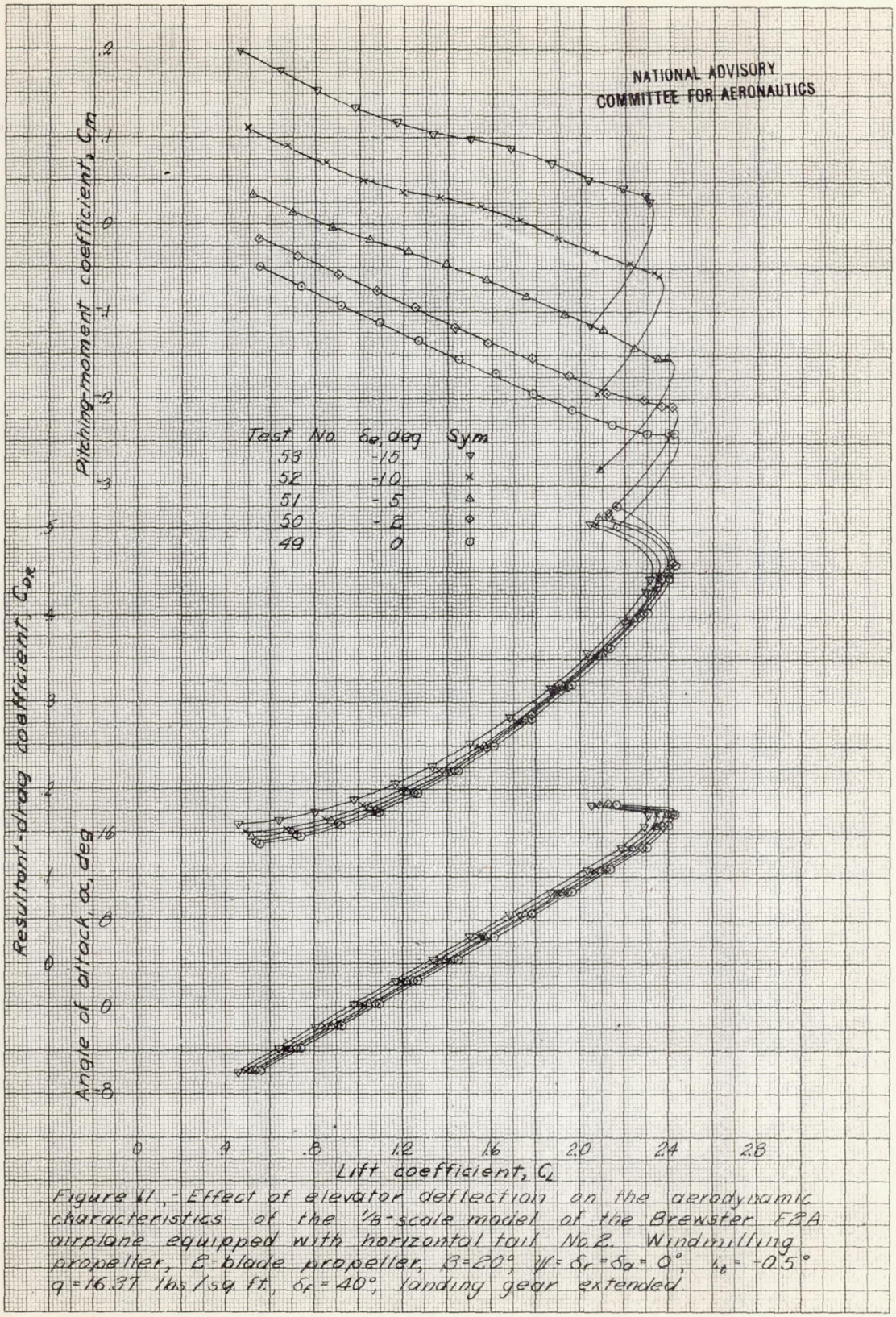

Figure 11.- Effect of elevator deflection on the aerodynamic characteristics of the 1/8-scale model of the Brewster F2A airplane equipped with horizontal tail No. 2. Windmilling propeller, 2-blade propeller, β=20°; $\psi = \delta_r = \delta_a = 0°$; $i_t = -0.5°$; q=16.37 lbs/sq ft; δ_f=40°; landing gear extended.

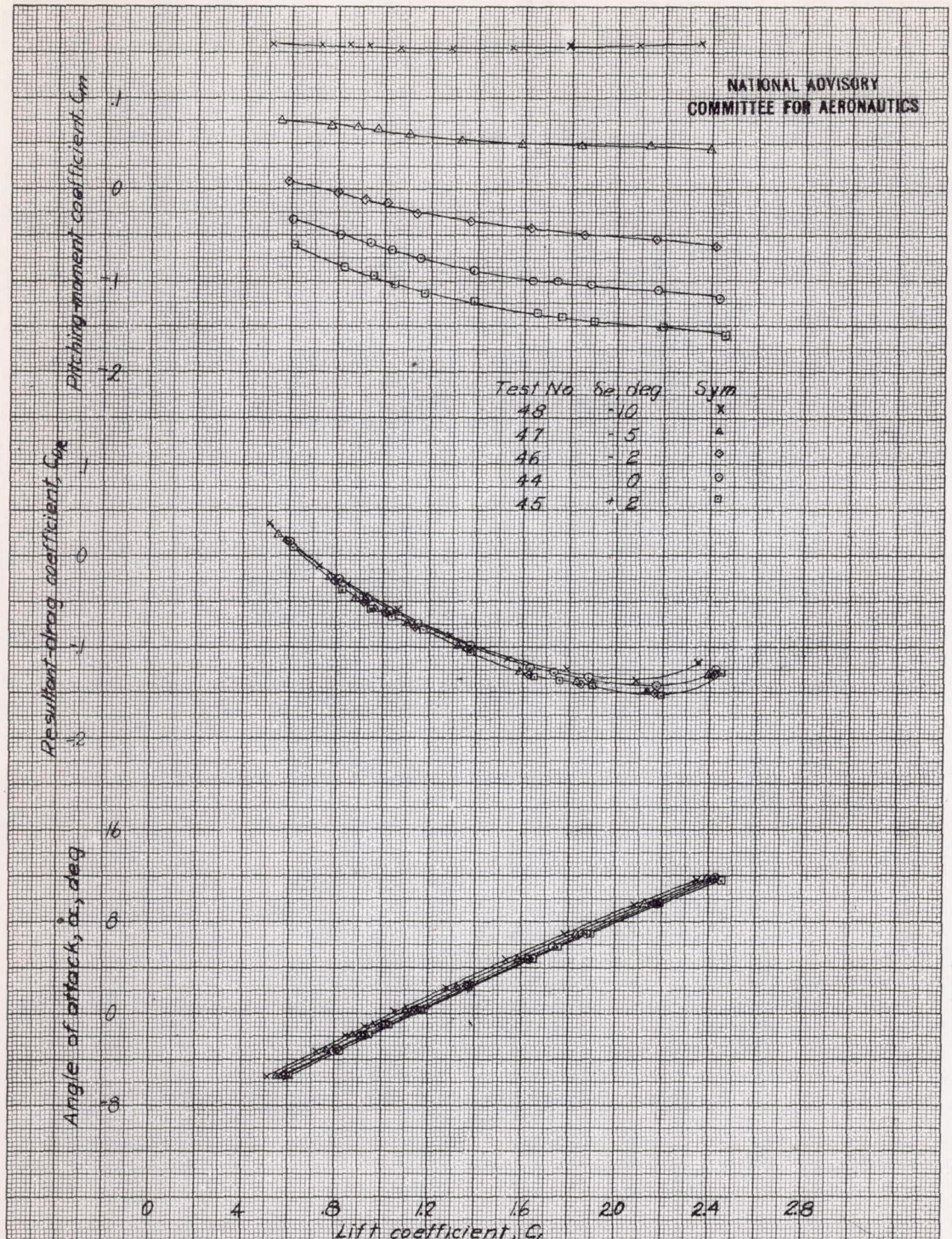

Figure 12.- Effect of elevator deflection on the aerodynamic characteristics of the 1/8-scale model of the Brewster F2A airplane equipped with horizontal tail No. 2. Approximately 1/2 rated power, 2-blade propeller, $\beta = 20°$; $\psi = \delta_r = \delta_a = 0$, $i_t = -0.5°$, $q = 16.27$ lbs/sq ft, $\delta_f = 40°$, landing gear extended.

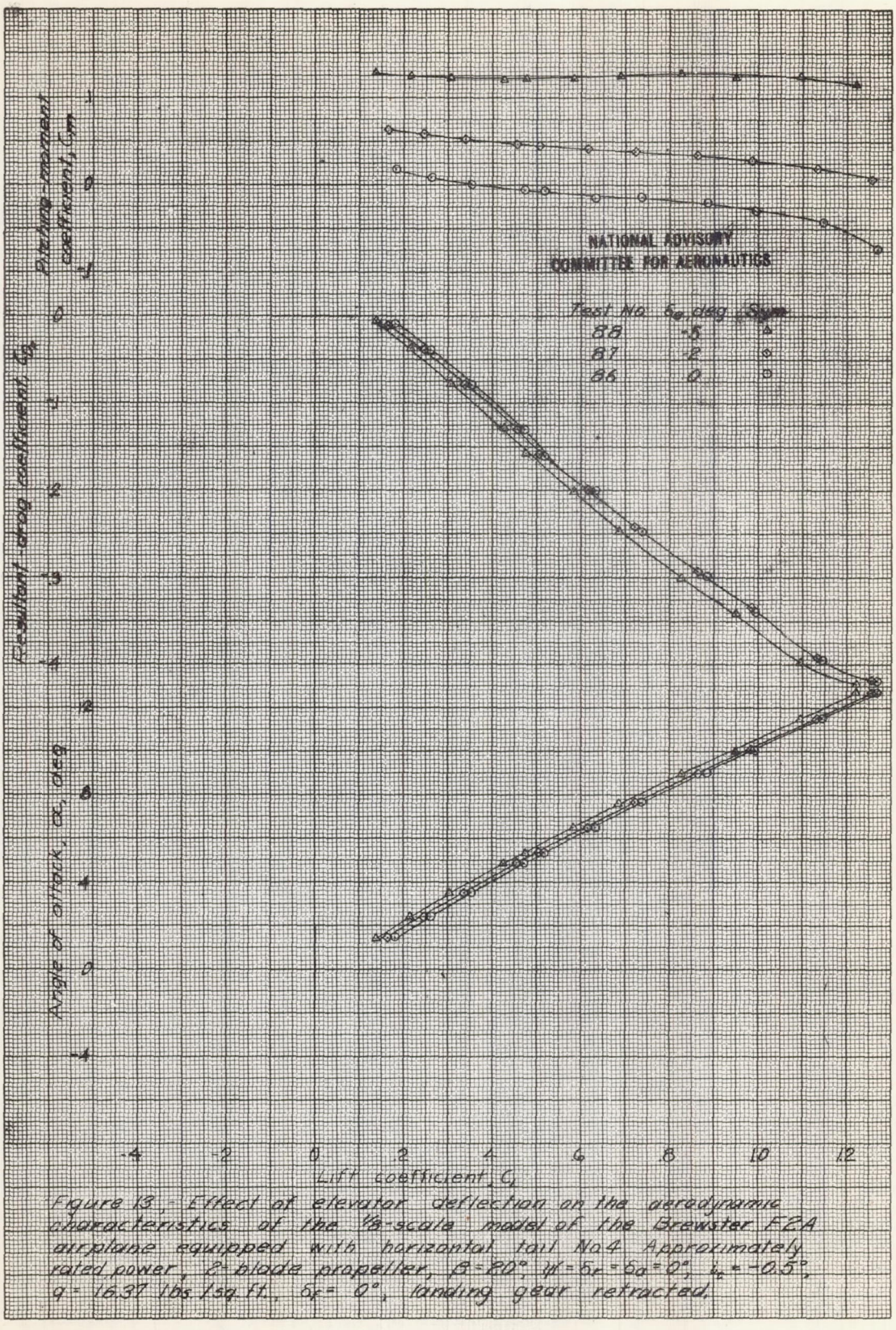

Figure 13. - Effect of elevator deflection on the aerodynamic characteristics of the 1/8-scale model of the Brewster F2A airplane equipped with horizontal tail No.4. Approximately rated power, 2-blade propeller, $\beta = 20°$, $i_t = \delta_r = \delta_a = 0°$, $i_w = -0.5°$, $q = 16.37$ lbs/sq ft., $\delta_f = 0°$, landing gear retracted.

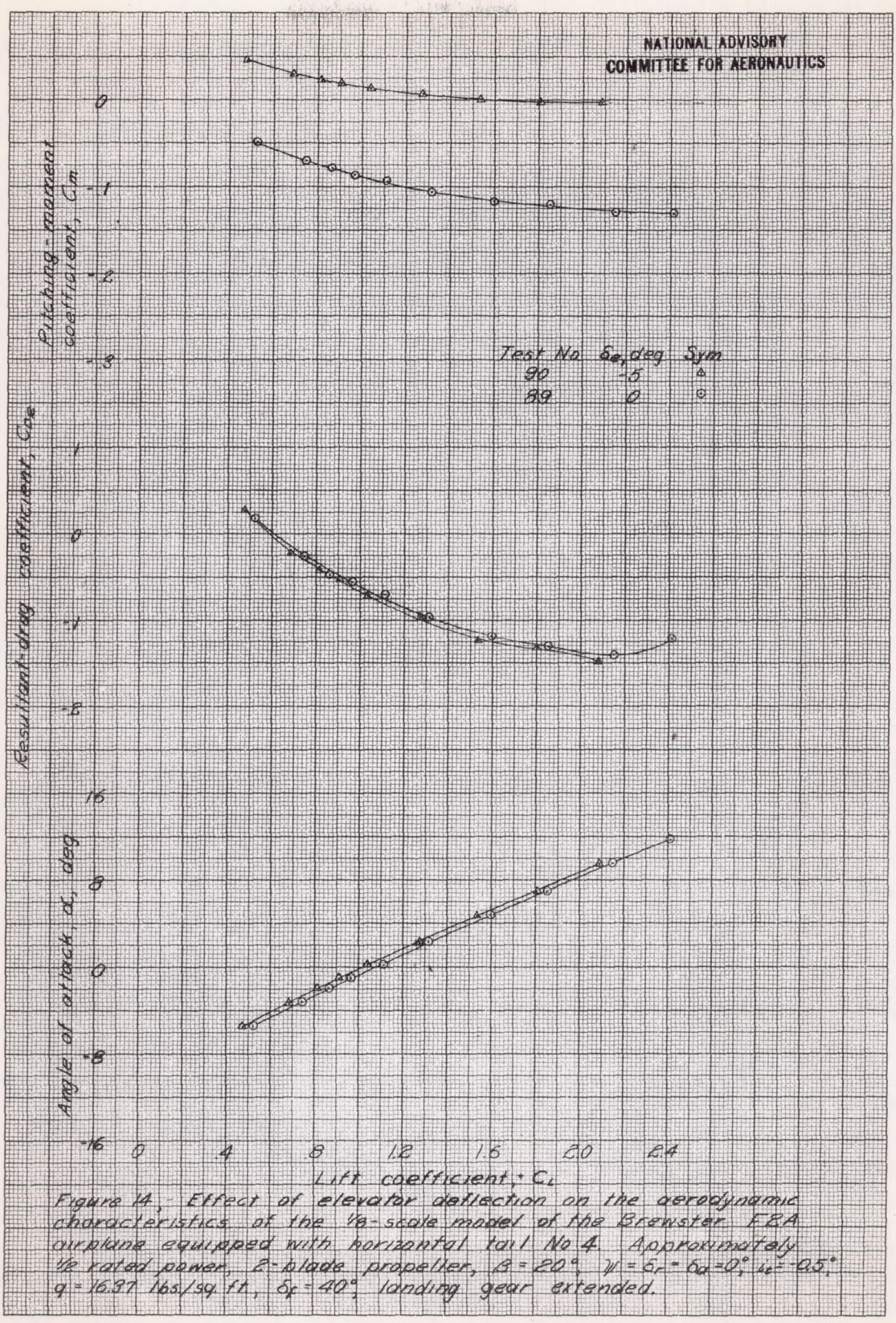

Figure 14. Effect of elevator deflection on the aerodynamic characteristics of the 1/8-scale model of the Brewster F2A airplane equipped with horizontal tail No 4. Approximately 1/2 rated power, 2-blade propeller, $\beta = 20°$, $\psi = \delta_r = \delta_a = 0°$, $i_t = -0.5°$, $q = 16.37$ lbs/sq ft, $\delta_f = 40°$, landing gear extended.

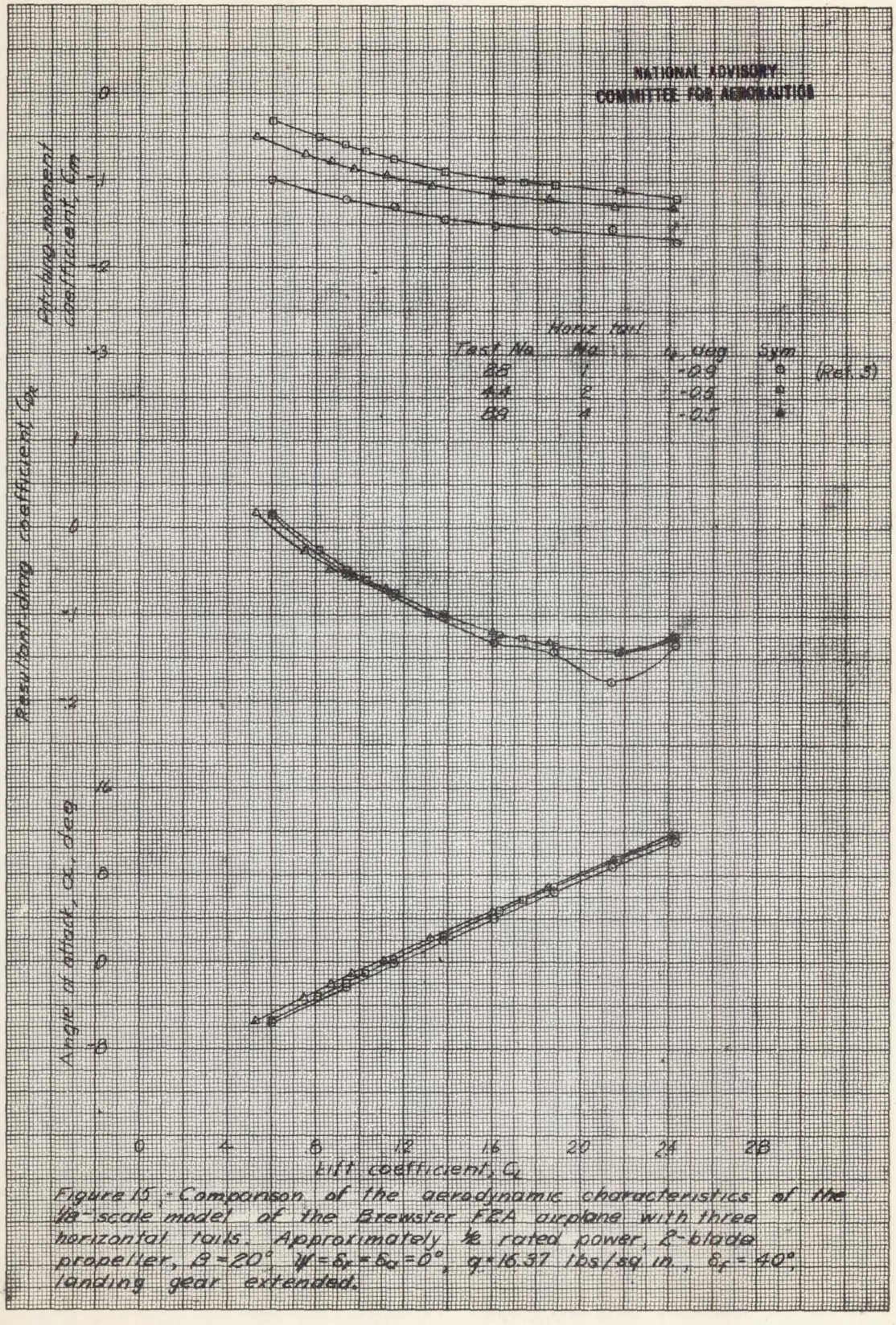

Figure 15 - Comparison of the aerodynamic characteristics of the 1/8-scale model of the Brewster F2A airplane with three horizontal tails. Approximately 1/2 rated power, 2-blade propeller, $\beta = 20°$, $i_w = \delta_f = \delta_a = 0°$, $q = 16.37$ lbs/sq in., $\delta_f = 40°$, landing gear extended.

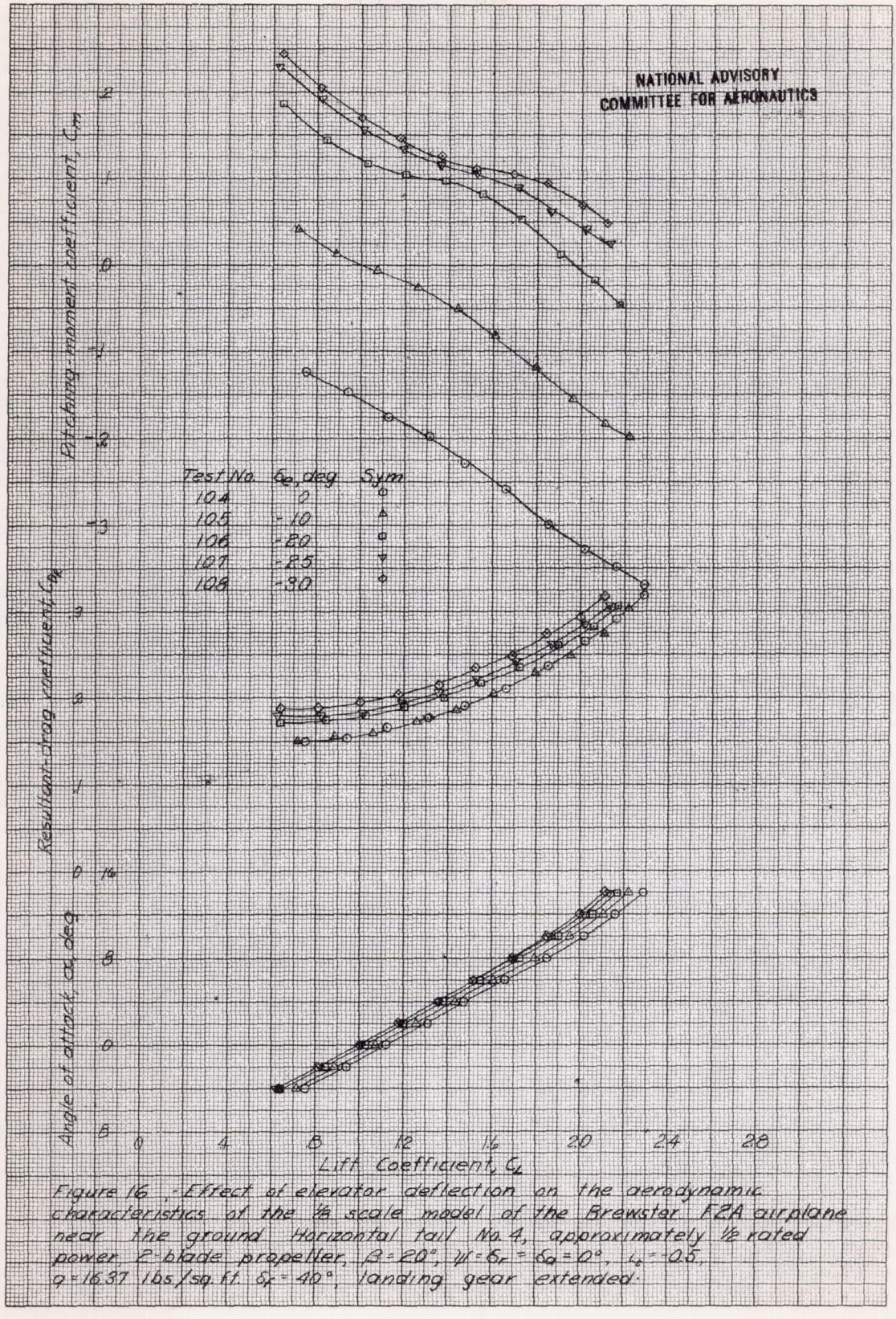

Figure 16 - Effect of elevator deflection on the aerodynamic characteristics of the 1/8 scale model of the Brewster F2A airplane near the ground. Horizontal tail No. 4, approximately 1/2 rated power, 2-blade propeller, $\beta = 20°$, $i_t = \delta_r = \delta_a = 0°$, $i_w = -0.5$, $q = 16.37$ lbs./sq. ft. $\delta_f = 40°$, landing gear extended.

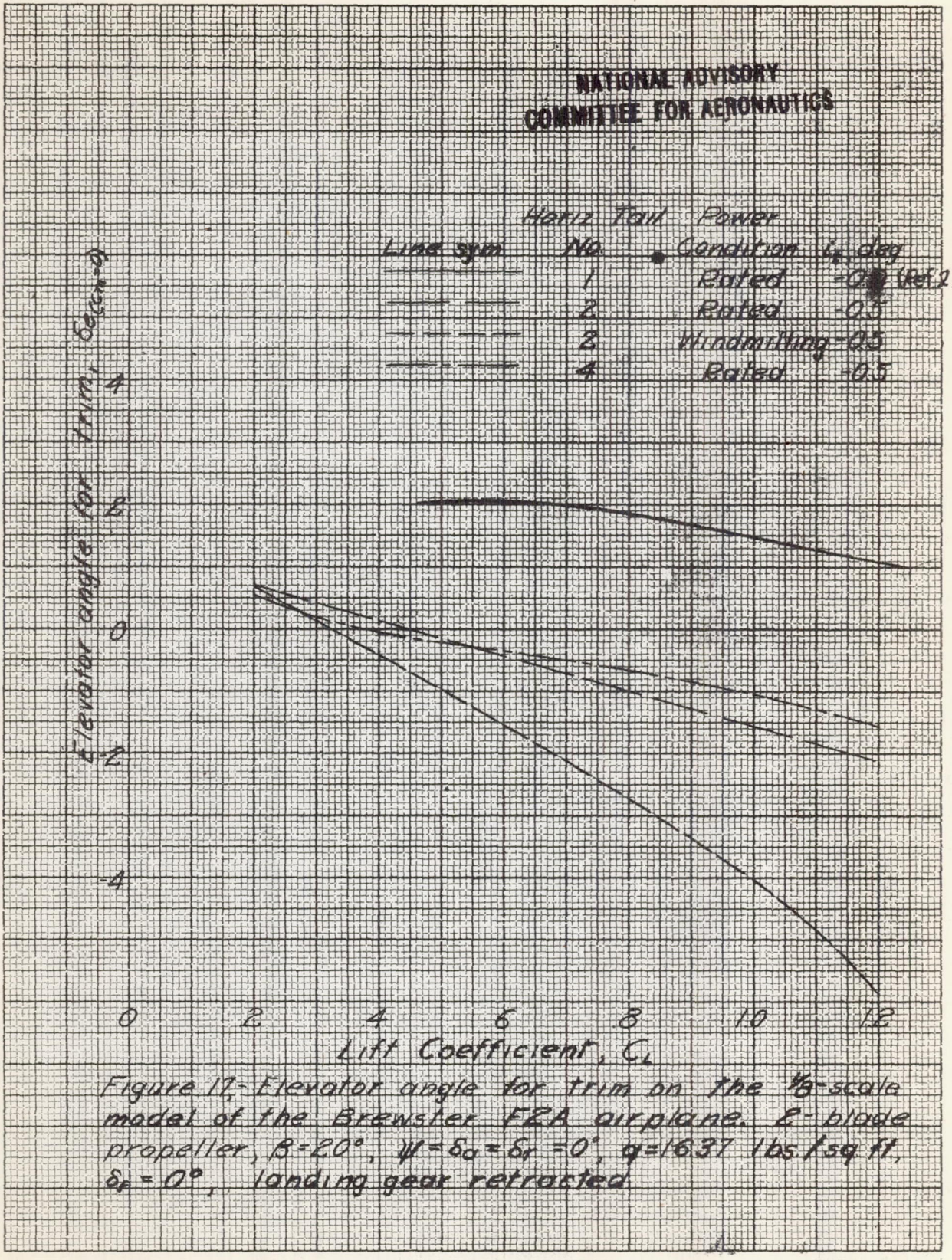

Figure 17.- Elevator angle for trim on the 1/8-scale model of the Brewster FZA airplane. 2-blade propeller, $\beta = 20°$, $\psi = \delta_a = \delta_r = 0°$, $q = 16.37$ lbs./sq ft., $\delta_f = 0°$, landing gear retracted.

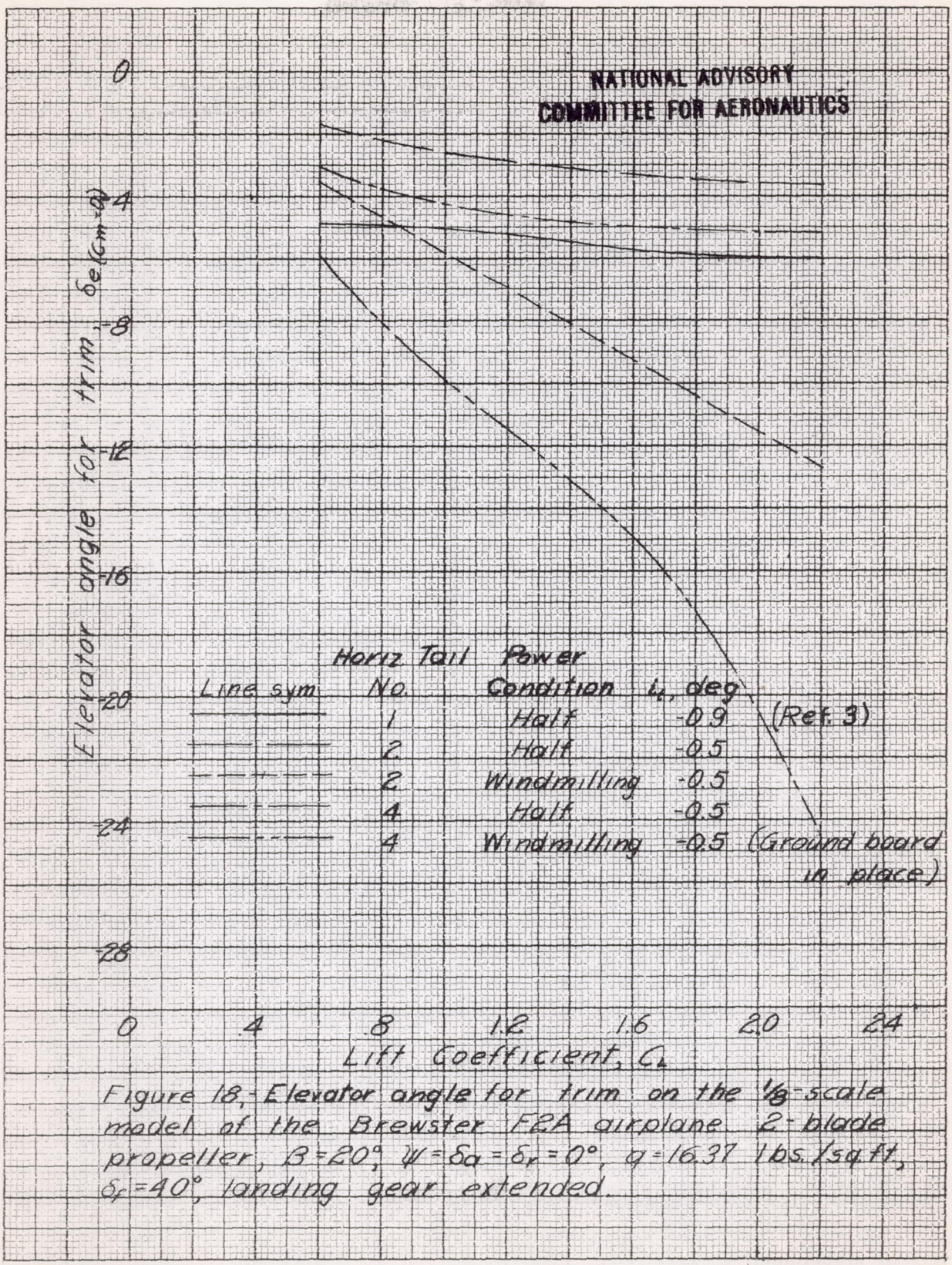

Figure 18.- Elevator angle for trim on the 1/8-scale model of the Brewster F2A airplane. 2-blade propeller, $\beta = 20°$; $\psi = \delta_a = \delta_r = 0°$, $q = 16.37$ lbs./sq.ft., $\delta_f = 40°$, landing gear extended.

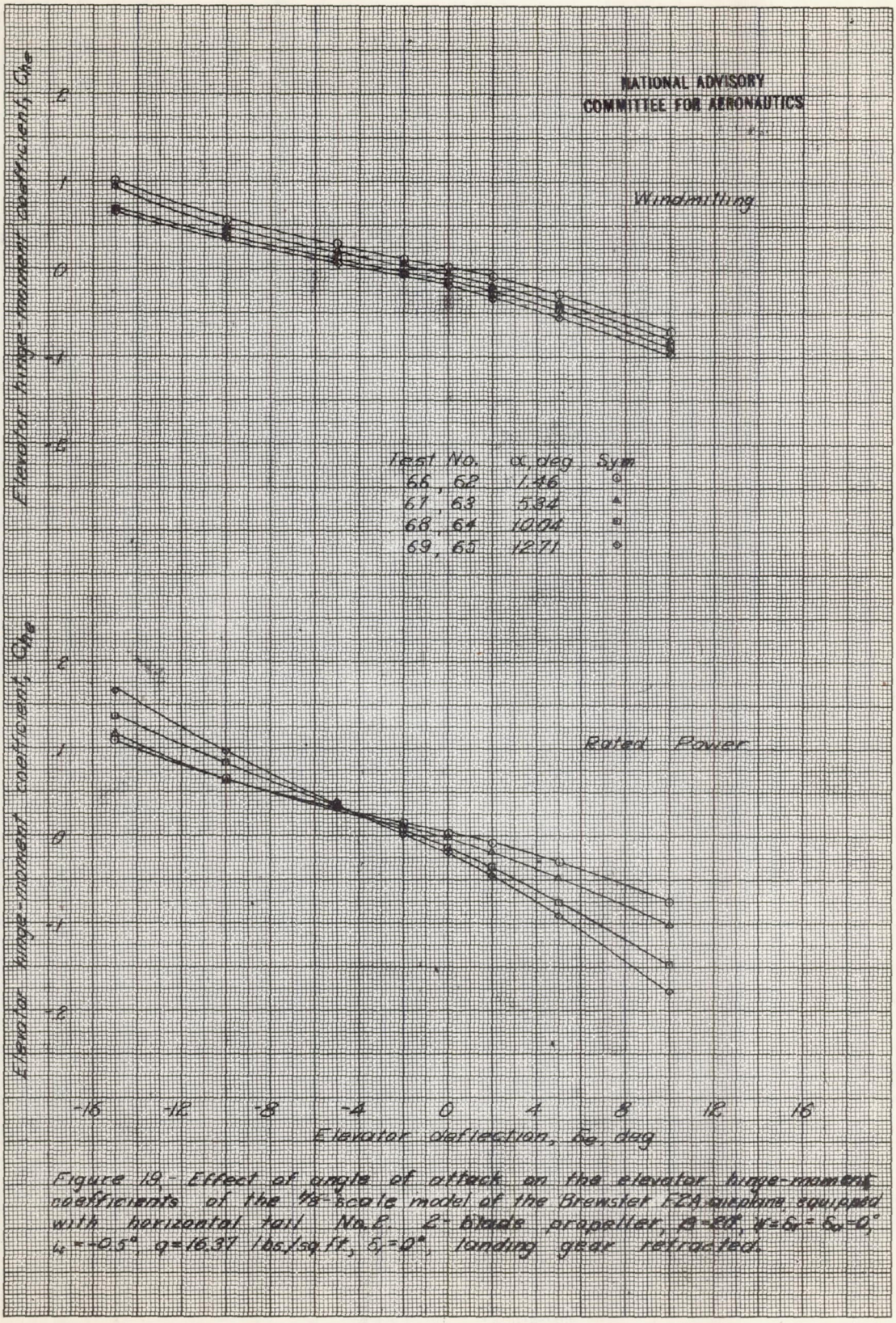

Figure 19.- Effect of angle of attack on the elevator hinge-moment coefficients of the 1/5-scale model of the Brewster XF2A airplane equipped with horizontal tail No.2. 2-blade propeller, i_t=-2°, ψ=δ_t=δ_a=0°, i_t=-0.5°, q=16.37 lbs/sq ft, δ_f=0°, landing gear retracted.

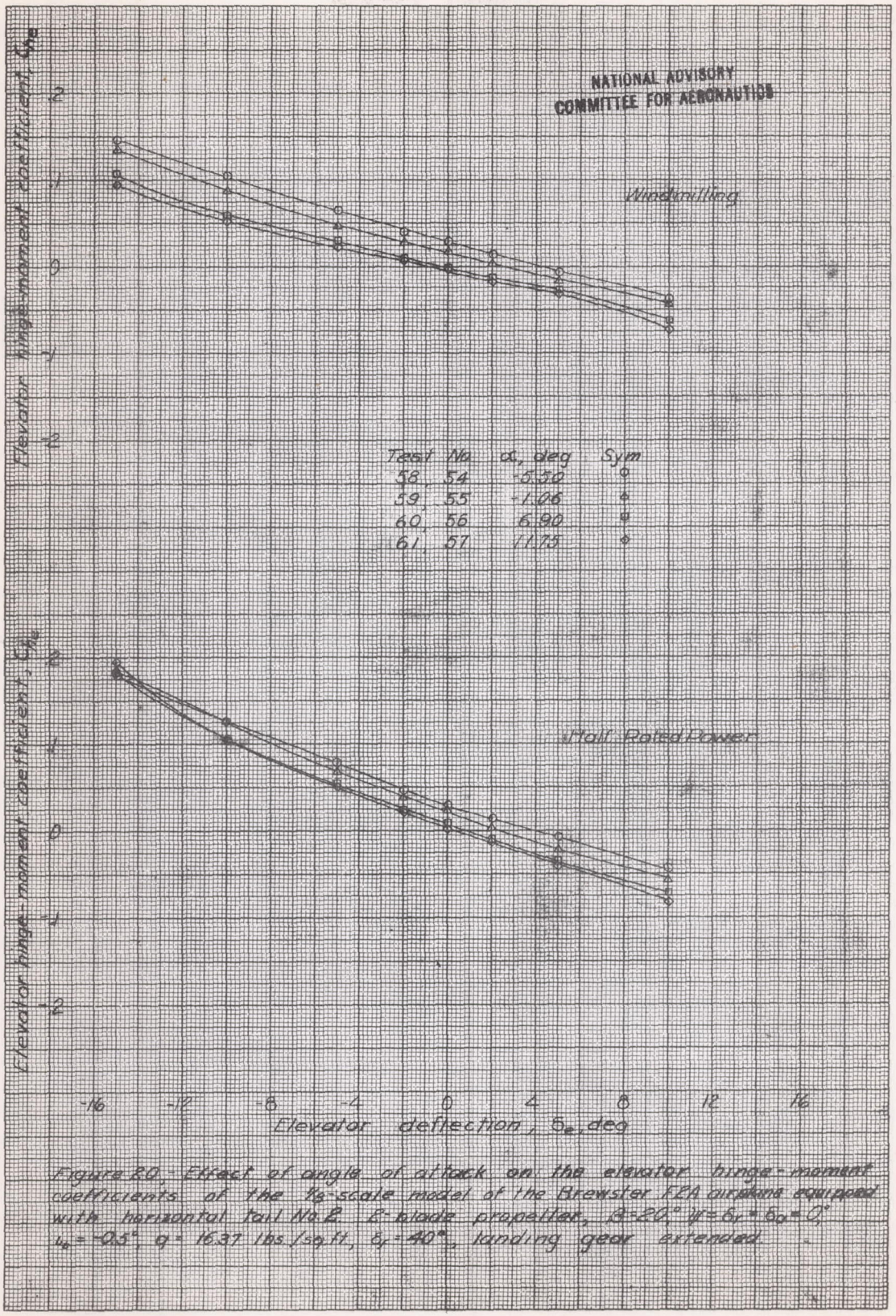

Figure 20. Effect of angle of attack on the elevator hinge-moment coefficients of the $\frac{1}{3}$-scale model of the Brewster FEA airplane equipped with horizontal tail No. 2. 2-blade propeller, $\beta = 20°$, $i_t = \delta_f = \delta_a = 0°$, $i_w = -0.5°$, $q = 16.37$ lbs/sq ft, $\delta_f = 40°$, landing gear extended.

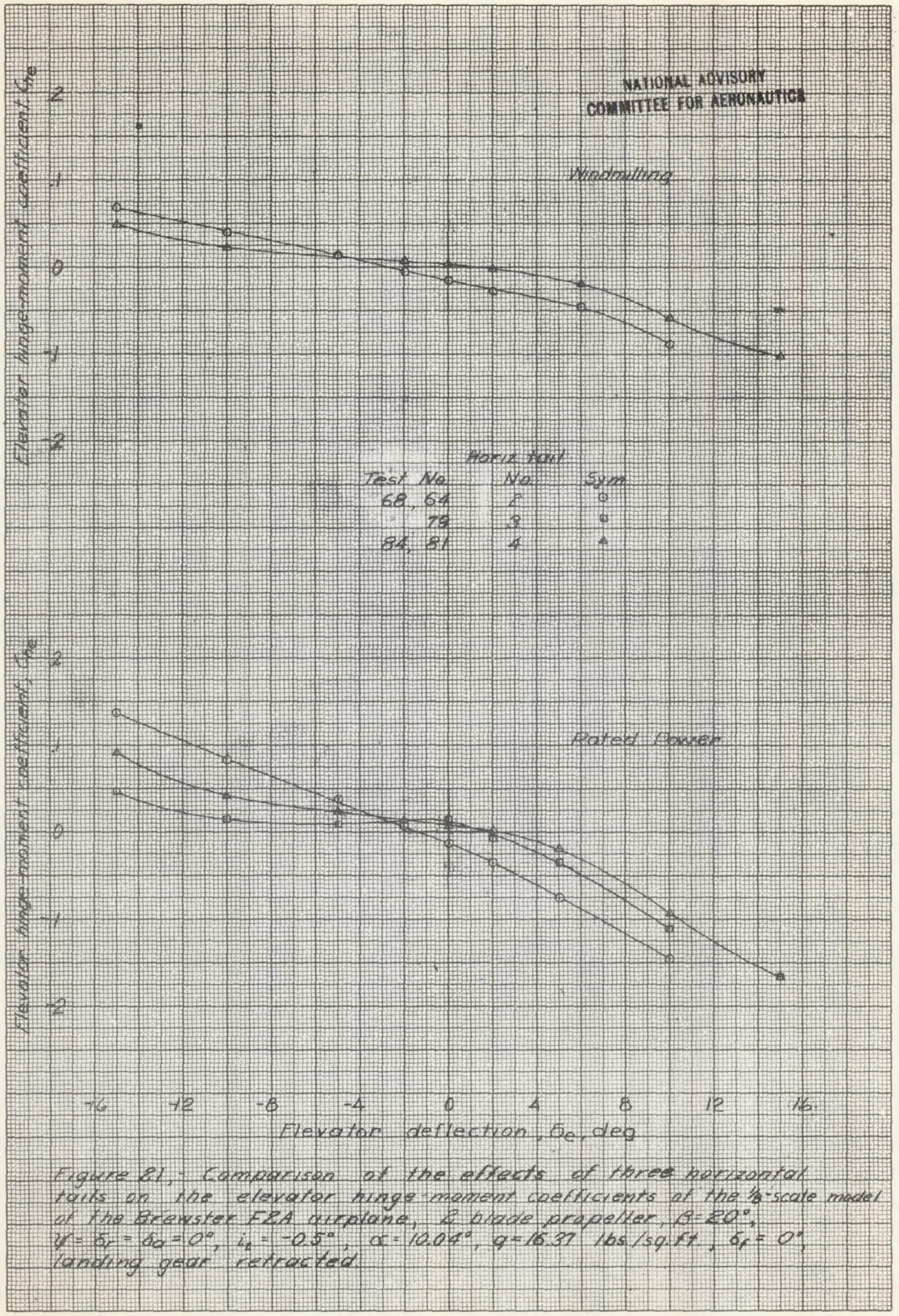

Figure 21.- Comparison of the effects of three horizontal tails on the elevator hinge-moment coefficients of the ½-scale model of the Brewster F2A airplane, 2 blade propeller, $\beta = 20°$, $\psi = \delta_r = \delta_a = 0°$, $i_t = -0.5°$, $\alpha = 10.04°$, $q = 16.37$ lbs/sq.ft., $\delta_f = 0°$, landing gear retracted.

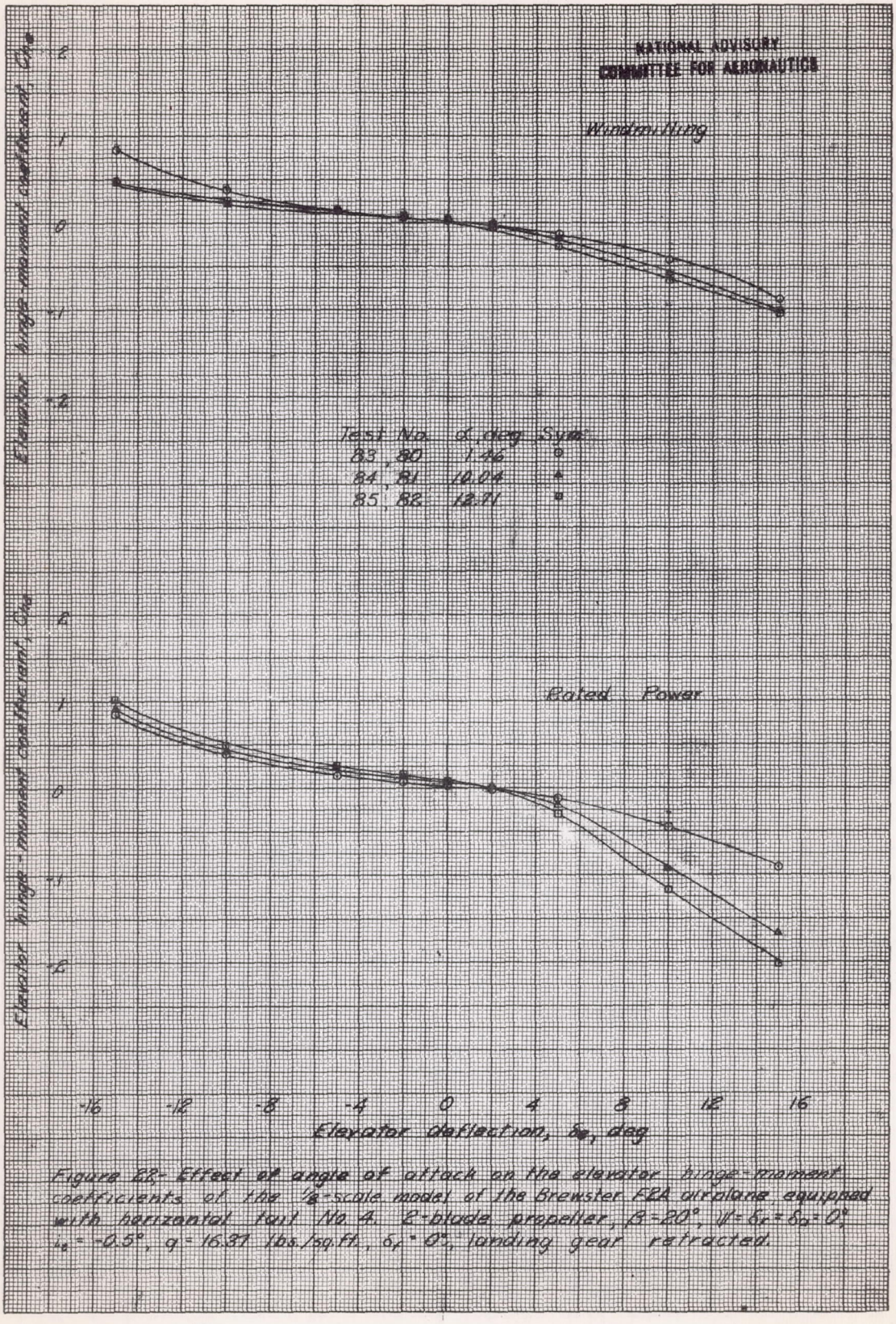

Figure 22.- Effect of angle of attack on the elevator hinge-moment coefficients of the 1/8-scale model of the Brewster F2A airplane equipped with horizontal tail No. 4. 2-blade propeller, $\beta = 20°$; $\psi = \delta_f = \delta_a = 0°$; $i_t = -0.5°$, $q = 16.31$ lbs./sq.ft., $\delta_f = 0°$, landing gear retracted.

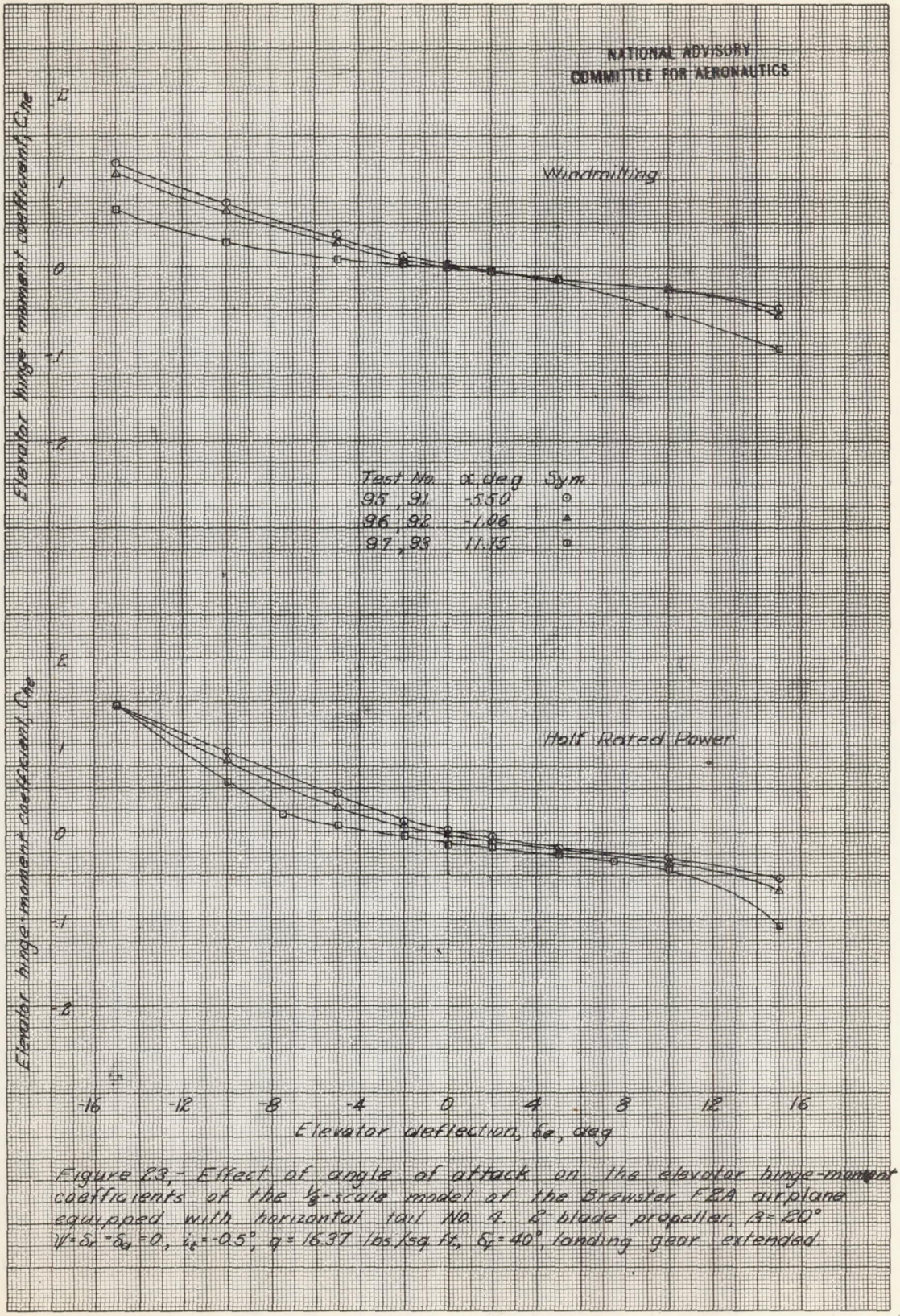

Figure 23.- Effect of angle of attack on the elevator hinge-moment coefficients of the ½-scale model of the Brewster F2A airplane equipped with horizontal tail No. 4, 2 blade propeller, $\beta = 20°$, $\delta_r = \delta_a = 0$, $i_t = -0.5°$, $q = 16.37$ lbs/sq ft, $\delta_f = 40°$, landing gear extended.

L-709

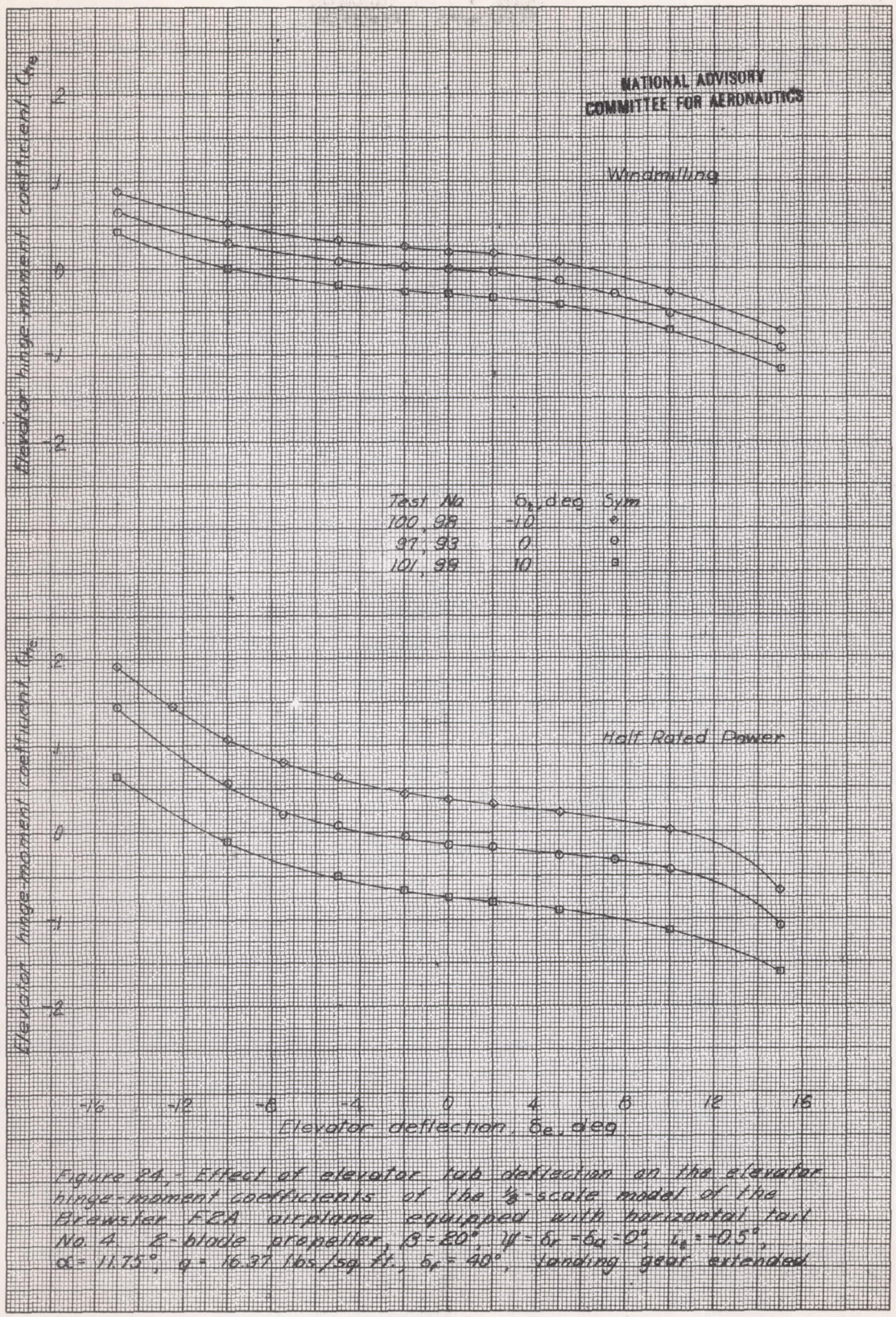

Figure 24.- Effect of elevator tab deflection on the elevator hinge-moment coefficients of the 1/3-scale model of the Brewster F2A airplane equipped with horizontal tail No. 4, 2-blade propeller, $\beta = 20°$, $i_f = \delta_f = \delta_a = 0°$, $i_a = +0.5°$, $\alpha = 11.75°$, $q = 16.37$ lbs/sq ft., $\delta_f = 40°$, landing gear extended.

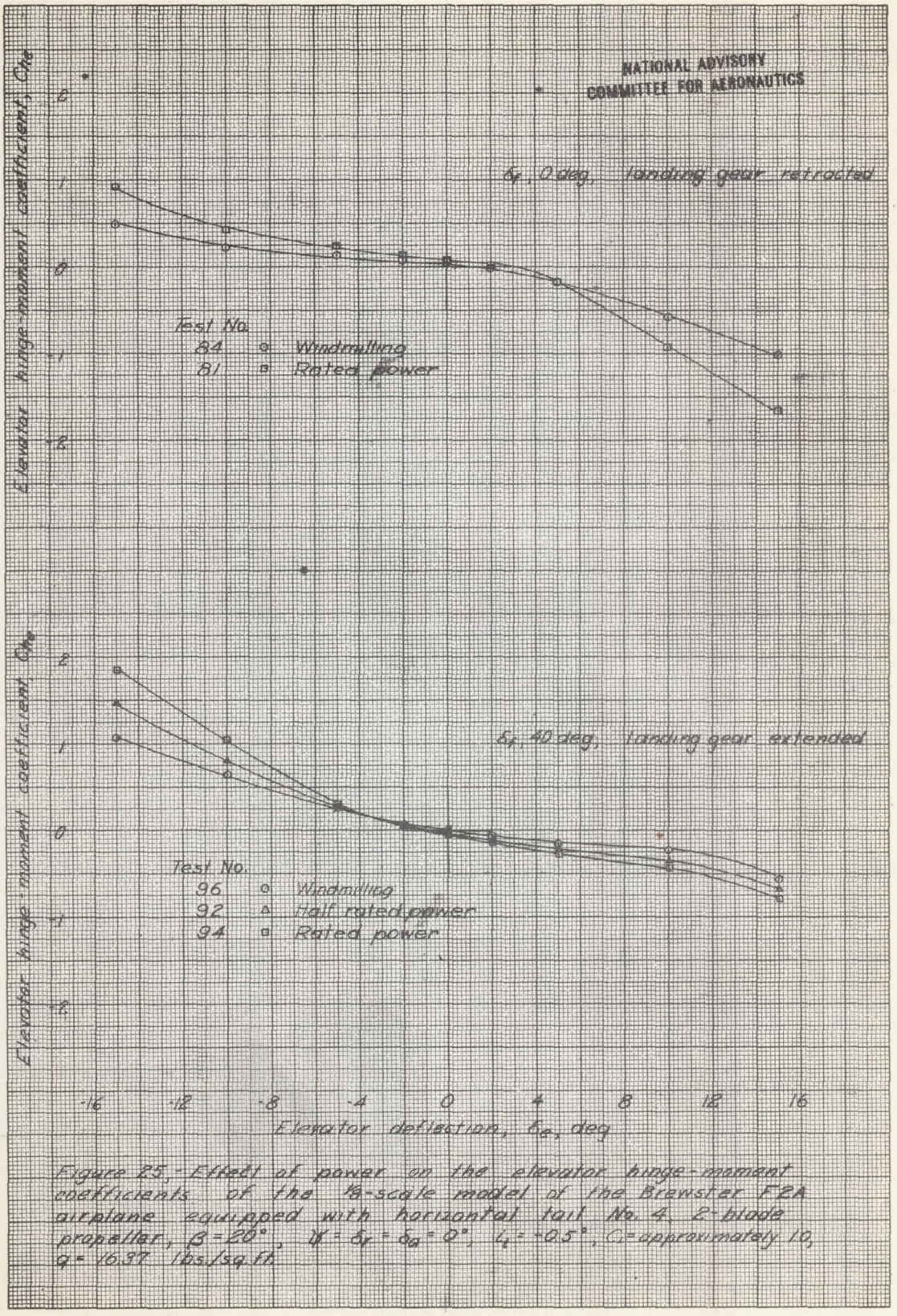

Figure 25.- Effect of power on the elevator hinge-moment coefficients of the 1/8-scale model of the Brewster F2A airplane equipped with horizontal tail No. 4, 2-blade propeller, $\beta = 20°$, $i_t = \delta_f = \delta_a = 0°$, $i_t = -0.5°$, C.G. approximately 10, $q = 16.37$ lbs/sq ft.

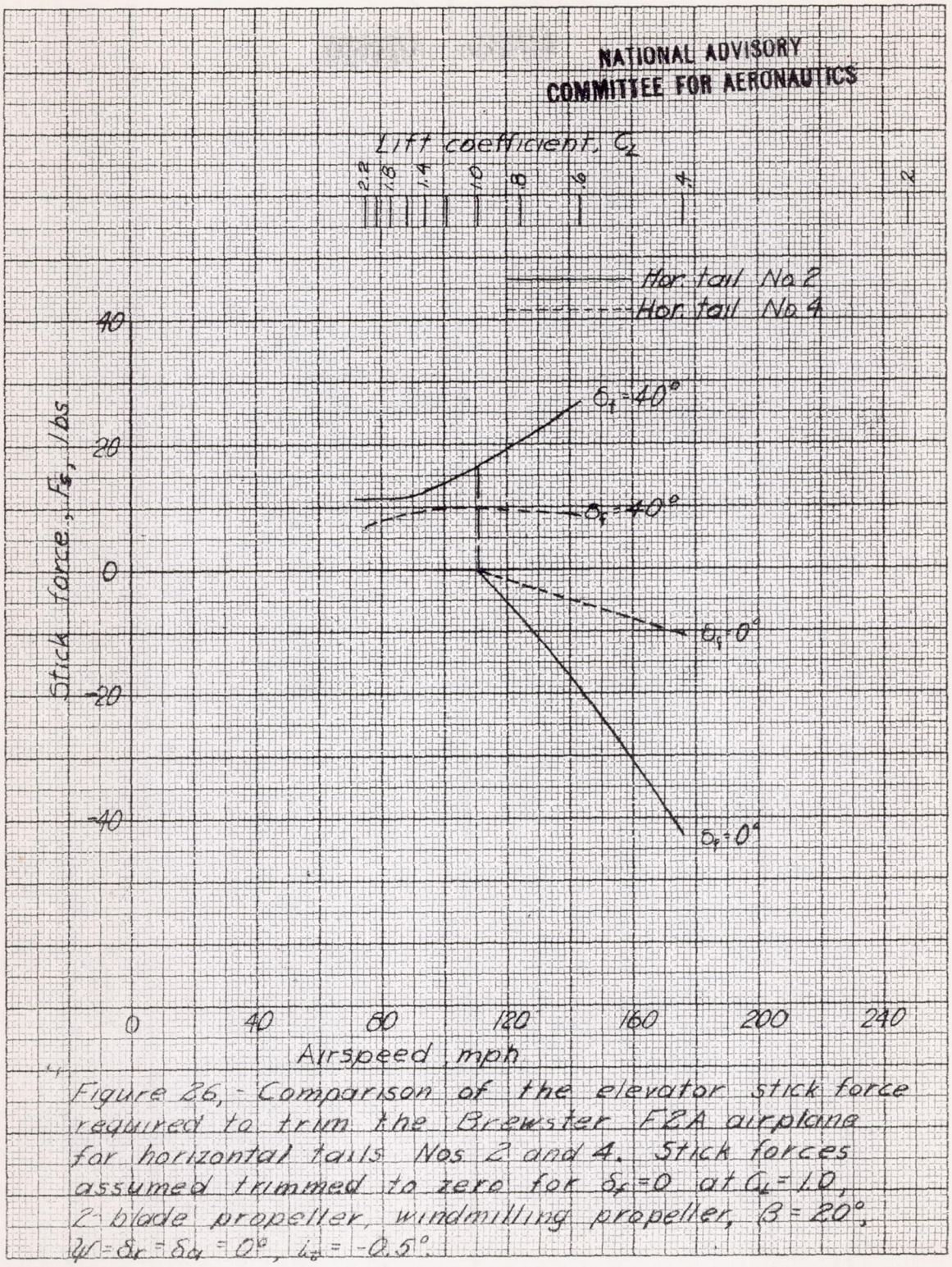

Figure 26.- Comparison of the elevator stick force required to trim the Brewster F2A airplane for horizontal tails Nos. 2 and 4. Stick forces assumed trimmed to zero for $\delta_t = 0$ at $C_L = 1.0$, 2-blade propeller, windmilling propeller, $\beta = 20°$, $\psi = \delta_r = \delta_a = 0°$, $i_t = -0.5°$.